

# LIBERO-Para: A Diagnostic Benchmark and Metrics for Paraphrase Robustness in VLA Models

Chanyoung Kim<sup>1\*</sup> Minwoo Kim<sup>1\*</sup> Minseok Kang<sup>1</sup> Hyunwoo Kim<sup>2</sup> Dahuin Jung<sup>2†</sup>

<sup>1</sup>Soongsil University <sup>2</sup>Chung-Ang University

{verddak, alsdn5531, alstjrrkd201}@soongsil.ac.kr, {k980814h, dahuinjung}@cau.ac.kr

## Abstract

Vision–Language–Action (VLA) models achieve strong performance in robotic manipulation by leveraging pre-trained vision–language backbones. However, in downstream robotic settings, they are typically fine-tuned with limited data, leading to overfitting to specific instruction formulations and leaving robustness to paraphrased instructions underexplored. To study this gap, we introduce LIBERO-Para, a controlled benchmark that independently varies action expressions and object references for fine-grained analysis of linguistic generalization. Across seven VLA configurations (0.6B–7.5B), we observe consistent performance degradation of 22–52 pp under paraphrasing. This degradation is primarily driven by object-level lexical variation: even simple synonym substitutions cause large drops, indicating reliance on surface-level matching rather than semantic grounding. Moreover, 80–96% of failures arise from planning-level trajectory divergence rather than execution errors, showing that paraphrasing disrupts task identification. Binary success rate treats all paraphrases equally, obscuring whether models perform consistently across difficulty levels or rely on easier cases. To address this, we propose PRIDE, a metric that quantifies paraphrase difficulty using semantic and syntactic factors. Our benchmark and corresponding code are available at: <https://github.com/cau-hai-lab/LIBERO-Para>

## 1 Introduction

Vision–Language–Action (VLA) models have emerged as a promising paradigm for robotic manipulation (Zitkovich et al., 2023; Black et al., 2024). By leveraging large pre-trained vision–language models (VLMs) as backbones, VLA models acquire instruction-following capabilities through large-scale multimodal percep-

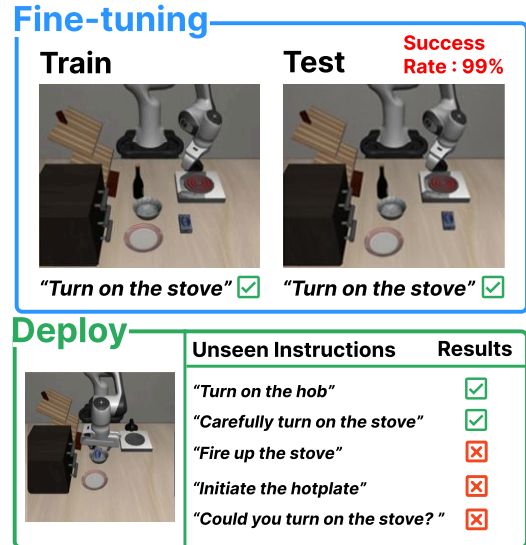


Figure 1: Illustration of paraphrase robustness gap under data-scarce fine-tuning: VLA models can overfit to seen instruction phrasings during fine-tuning and fail to generalize to paraphrased variants at deployment.

tion (Zitkovich et al., 2023; Black et al., 2024). To deploy such models in specific environments (e.g., kitchens, homes, offices, or laundry rooms) (Black et al., 2024; Physical Intelligence et al., 2025; Zitkovich et al., 2023; Fu et al., 2024; Wu et al., 2023), existing approaches typically perform fine-tuning using environment-specific demonstration data (Fu et al., 2024). However, acquiring such data entails considerable cost and labor overhead. Consequently, real-world deployment often necessitates data-scarce fine-tuning, which can induce overfitting and degrade the general knowledge embedded in pre-trained VLA models (Yadav et al., 2025; Zhou et al., 2025). Such overfitting raises a practical concern that models may perform well on seen instruction phrasings yet fail to generalize to unseen paraphrased instructions at deployment. Under these circumstances, as shown in Fig. 1, benchmarks that rigorously assess robustness after fine-tuning become important (Zhou et al., 2025).

\* Equal contribution. † Corresponding author.

However, the LIBERO benchmark (Liu et al., 2023), which has become widely adopted in current VLA research, evaluates models under identical instructions during both training and evaluation. It primarily measures visual generalization to novel object configurations or scene layouts, while leaving robustness to linguistic variation largely unexamined. Consequently, the linguistic robustness of VLA models remains insufficiently validated (Fei et al., 2025; Wang et al., 2024; Zhou et al., 2025).

Several benchmarks have examined linguistic variation in VLA evaluation (Mees et al., 2021; Wang et al., 2024). However, as summarized in Tab. 1, these approaches exhibit key limitations for assessing paraphrase robustness. Paraphrasing is often treated as one axis among broader multimodal perturbations (Zhou et al., 2025; Fei et al., 2025; Wang et al., 2026), or conflated with task-level semantic changes that alter the intended behavior (Hou and Zhao, 2026), rather than isolating meaning-preserving variation. Furthermore, linguistic properties specific to robotic manipulation instructions are not explicitly modeled, and the distance between paraphrases is not formally quantified, limiting the ability to analyze which types of variation most severely impact performance.

To address these limitations, we introduce LIBERO-Para, a controlled benchmark for evaluating paraphrase robustness in VLA models, along with PRIDE (Paraphrase Robustness Index in Robotic Instructional DEviation), a metric that combines keyword similarity (lexical shift) and structural similarity (syntactic variation) with task success to enable fine-grained robustness analysis. LIBERO-Para is grounded in the linguistic structure of robotic manipulation instructions—where actions and objects serve as core semantic elements—and adopts a two-axis design that independently varies action expressions and object references. Our analysis based on LIBERO-Para reveals three key findings:

- **Paraphrase Fragility Persists:** Performance consistently degrades under paraphrased instructions across architectures, scales, and fine-tuning strategies.
- **Object-Level Bottleneck:** Object-level lexical variation is the dominant source of degradation, indicating reliance on surface-level matching rather than semantic grounding.
- **Planning-Level Failures:** 80–96% of failures

Benchmark	Scope	Paraphrase Control	Variation Axis	Para. Types
CALVIN	Instruction	×	Sentence	1
LADEV	Paraphrase	×	Sentence	1
LIBERO-PRO	Multimodal	△	Sentence	2
LIBERO-Plus	Multimodal	△	Sentence	5
LIBERO-X	Multimodal	△	Sentence	5
LangGap	Task Semantics	×	4 Semantic dims	4
LIBERO-Para (Ours)	Paraphrase	✓	Action × Object	43

Table 1: Comparison with existing benchmarks for linguistic robustness. LIBERO-Para provides full paraphrase control with fine-grained action × object variation axes and 43 linguistically grounded types. ×: not supported, △: partially supported, ✓: fully supported.

arise from trajectory divergence, suggesting errors in task identification rather than action execution.

This work contributes to advancing VLA systems beyond high performance toward robustness to linguistic variation and reliable task interpretation.

## 2 Related Work

### 2.1 Vision-Language-Action Models

Vision-Language-Action (VLA) models map visual and linguistic input to robot actions. Early approaches extend LLM backbones to autoregressively decode discrete action tokens (Zitkovich et al., 2023; Kim et al., 2024). Recent work has diversified along several architectural axes: parallel decoding with action chunking, which predicts all actions in a single forward pass for faster inference (Kim et al., 2025); VLM coupled with a flow-matching action expert, which pairs a billion-scale VLM with a separate action decoder (Black et al., 2024; Physical Intelligence et al., 2025; Cai et al., 2026); lightweight bridge-based adaptation, which routes VLM representations to a compact policy head via cross-attention (Wang et al., 2025); and soft-prompted cross-embodiment designs, which encode embodiment-specific knowledge through learnable tokens (Zheng et al., 2025). The latter two operate at 0.6–0.9B scale, contrasting with earlier multi-billion-parameter designs. Despite this diversity, all models require environment-specific fine-tuning with limited demonstration data. In this work, we evaluate representatives from each family to assess whether paraphrase robustness is an architecture-specific issue or a shared vulnerability.

### 2.2 Benchmarks for VLA models

A range of benchmarks have been proposed to evaluate linguistic conditioning in VLA models; Tab. 1 compares their design choices. CALVIN (Mees

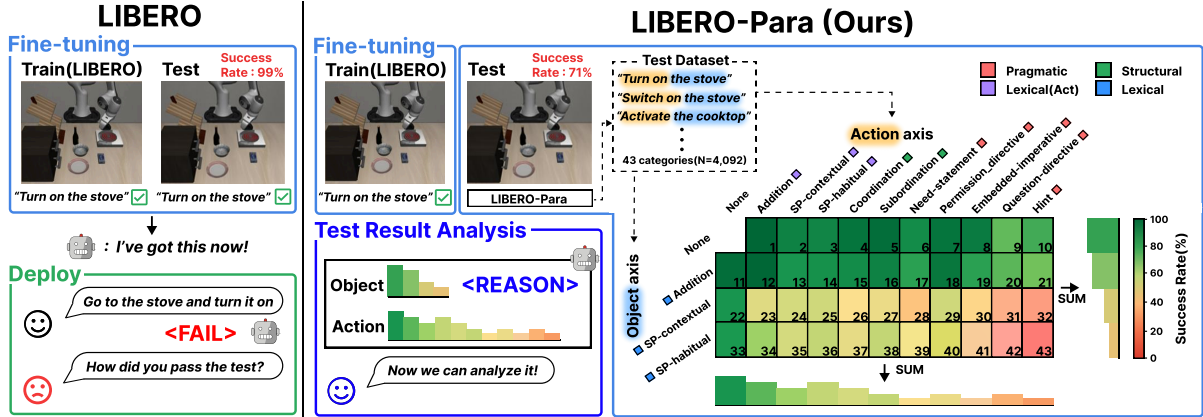


Figure 2: Overview of LIBERO-Para. Compared to LIBERO, LIBERO-Para evaluates paraphrase robustness under data-scarce fine-tuning via a controlled two-axis design (action vs. object), enabling interpretable analysis.

et al., 2021) and LADEV (Wang et al., 2024) assess generalization to rephrased instructions, but treat paraphrasing as unstructured sentence-level variation without linguistic categorization. LIBERO-PRO, LIBERO-Plus, and LIBERO-X (Zhou et al., 2025; Fei et al., 2025; Wang et al., 2026) introduce multimodal perturbation-based evaluations that include linguistic variation as one of several axes, revealing limited dependence on genuine linguistic understanding; however, paraphrasing remains a secondary concern within their broader evaluation scope. LangGap (Hou and Zhao, 2026) targets language conditioning more directly, but its perturbations alter the intended behavior (e.g., changing which object to grasp), conflating task-level semantic changes with linguistic variation. In contrast, our LIBERO-Para differs in two key aspects: (1) it isolates meaning-preserving linguistic variation from task-level semantic changes, and (2) rather than applying sentence-level perturbations with ad-hoc categories, it identifies the essential linguistic components of robotic manipulation instructions—action verbs and object references—and decomposes paraphrases along these two axes based on established linguistic taxonomies (Kovatchev et al., 2018; Ervin-Tripp, 1976), yielding 43 fine-grained variation types (Tab. 1).

### 3 LIBERO-Para: A Controlled VLA Benchmark for Paraphrase Robustness

We introduce LIBERO-Para, a controlled benchmark for evaluating the paraphrase robustness of VLA models. As shown in Tab. 1, existing benchmarks offer limited control over paraphrase variation; our design addresses this through a two-axis scheme that independently varies action expres-

sions and object references—the two core linguistic components of robotic manipulation instructions. This separation enables controlled analysis of how different linguistic factors affect VLA performance. LIBERO-Para is constructed on top of LIBERO-Goal, a setting in which linguistic understanding is essential: all tasks start from an identical initial state, making the instruction the sole cue for task identification. We generate the benchmark by paraphrasing only the instructions while keeping all other factors fixed. All paraphrases are held out for evaluation, allowing assessment of generalization to unseen linguistic variations under data-scarce fine-tuning scenarios, as illustrated in Fig. 2.

#### 3.1 Action Variation

The action axis captures variation in how actions are linguistically expressed. We define three types of action variation grounded in established paraphrase taxonomies. (1) Lexical variation modifies the action verb at the word level, including synonym substitution and adverb insertion. (2) Structural variation alters the sentence-level realization of the action expression, such as coordination and subordination. (3) Pragmatic variation expresses actions indirectly, covering indirect speech acts. Lexical and structural variations are instantiated based on the Extended Paraphrase Typology (Kovatchev et al., 2018). Pragmatic variations are defined in accordance with Ervin-Tripp (1976). Fig. 3 (bottom) presents representative examples for each type.

#### 3.2 Object Variation

captures variation in how objects are referenced in instructions. In robotic manipulation, object references are typically realized as noun phrases with

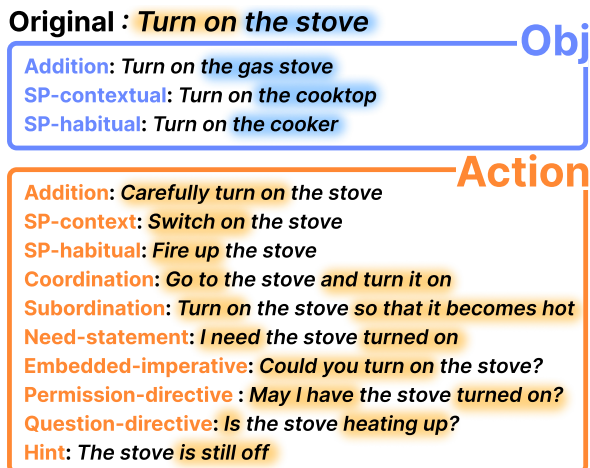


Figure 3: Examples of axis-specific paraphrases. Object variations modify target object references (e.g., same-polarity substitution, addition), while action variations cover lexical, structural, and pragmatic realizations grounded in established taxonomies.

limited complexity (e.g., “the stove” → “the cooktop”). We focus on lexical-level variation. Following the Extended Paraphrase Typology (Kovatchev et al., 2018), we define three subtypes: addition and same-polarity substitution (contextual and habitual variants). Fig. 3 (top) illustrates representative examples.

### 3.3 Compositional Variation

Beyond individual axes, we evaluate compositional paraphrases that vary both action and object expressions. This setting enables analysis of whether the two axes have independent or interaction effects on VLA performance. Fig. 2 presents an example, including a success-rate grid over variation combinations and success rates for each axis.

To ensure balanced evaluation, the benchmark includes approximately 100 samples per variation type, resulting in a total of 4,092 paraphrased instructions. Additional details on the taxonomy, paraphrase generation process, and excluded variation types—including justifications for why certain types are inapplicable to robotic manipulation instructions—are provided in Appendix A.

## 4 PRIDE: Paraphrase Robustness Index in Robotic Instructional DEviation

Existing VLA benchmarks rely on a binary success metric, assigning 1 if the robot completes the instructed task and 0 otherwise. However, this metric does not distinguish between easy and difficult paraphrases, obscuring whether performance reflects robust linguistic understanding or reliance on

simpler instruction variants.

To enable interpretable robustness evaluation, we propose PRIDE, a metric that quantifies the linguistic deviation between an original instruction and its paraphrase. Unlike general-purpose metrics, PRIDE is tailored to robotic instructions and decomposes paraphrase variation along two axes: (1) keyword variation and (2) structural variation.

### 4.1 Keyword Similarity $S_K$

Keyword similarity measures how much core keywords expressing actions and target objects are preserved between an original instruction and its paraphrase. Robotic manipulation instructions are typically structured around explicit actions and their corresponding objects, often following a canonical form such as “[ACT] the [OBJ]” (e.g., “pick up the bowl”). As a result, the intended behavior is often determined by a small set of task-critical tokens rather than by the sentence as a whole.

This property limits the usefulness of form-based NLP metrics for paraphrased robotic instructions. For example, n-gram metrics such as BLEU (Papineni et al., 2002) emphasize lexical overlap and may fail to distinguish paraphrases that preserve actions and objects but differ in expression, through synonym substitution or word-order variation. Function words can also cause superficial grammatical changes to overly influence similarity scores relative to action- or object-level semantics.

In our setting, the two sentences are given as a paraphrase pair. Thus, rather than reassessing overall semantic equivalence, it is more useful to analyze how task-critical components change. Accordingly, we define a keyword-level similarity that focuses on content words expressing actions and objects excluding function words.

Let  $O = \{o_1, \dots, o_n\}$  and  $P = \{p_1, \dots, p_m\}$  denote the sets of content words extracted from the original and paraphrased instructions, respectively. Each word is represented by an embedding  $e(\cdot)$  obtained from Sentence-BERT (Reimers and Gurevych, 2019). The keyword similarity  $S_K(O, P)$  is computed by matching each content word  $o_i$  in the original instruction to the most similar word in the paraphrase, measured by cosine similarity, and averaging over all  $o_i$ :

$$S_K(O, P) = \frac{1}{n} \sum_{i=1}^n \max_{j \in \{1, \dots, m\}} \cos(e(o_i), e(p_j)), \quad (1)$$

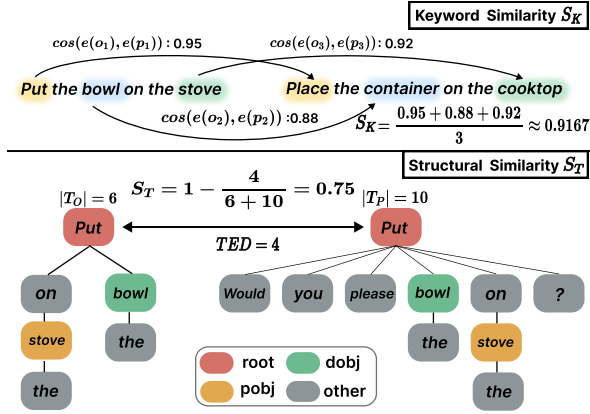


Figure 4:  $S_K$  (top) and  $S_T$  (bottom) computation.  $S_K$  is based on semantic matching between task-critical content words, while  $S_T$  uses dependency-tree edit distance. Node colors indicate dependency relations: root (sentence root), dobj (direct object), pobj (object of preposition), and others (remaining types, simplified for visualization; all included in computation).

where  $\cos(\cdot, \cdot)$  denotes cosine similarity. Fig. 4 (top) illustrates the computation of  $S_K$ . A higher value of  $S_K(O, P)$  indicates better preservation of the original instruction’s key content words in the paraphrase.

## 4.2 Structural Similarity $S_T$

While keyword similarity  $S_K$  captures the preservation of core lexical items, it does not account for syntactic changes. Transformations such as active-passive alternation or clause reordering can substantially alter the form of an instruction while preserving the same keywords. To capture such variation, we introduce structural similarity  $S_T$ .

We measure syntactic change using the tree edit distance (TED) (Augsten and Böhlen, 2013) between the dependency trees of the original and paraphrased instructions, denoted by  $T_O$  and  $T_P$ . TED is defined as the minimum number of edit operations—node and edge insertions, deletions, and substitutions—required to transform one tree into the other. To focus on structural differences, we compute TED on dependency trees whose node labels are part-of-speech (POS) tags and whose edge labels are dependency relations rather than surface words, reducing sensitivity to lexical substitutions.

To mitigate sentence-length effects, we normalize TED by the combined size of two trees and define structural similarity  $S_T(T_O, T_P)$  as follows:

$$S_T(T_O, T_P) = 1 - \frac{\text{TED}(T_O, T_P)}{|T_O| + |T_P|}. \quad (2)$$

where  $|\cdot|$  denotes the number of nodes in tree

Method	LIBERO-Goal SR	LIBERO-Para SR (Drop)
OpenVLA-OFT <sub>goal</sub>	97.9	64.7 (-33.2)
OpenVLA-OFT <sub>mixed</sub>	96.1	63.7 (-32.4)
$\pi_{0.5}$	97.6	71.4 (-26.2)
$\pi_{0.5}$ (expert-only)	78.6	39.1 (-39.5)
X-VLA	97.8	62.1 (-35.7)
VLA-Adapter	98.2	46.3 (-51.9)
Xiaomi-Robotics-0	98.8	76.0 (-22.8)

Table 2: Success rate (SR) comparison between LIBERO-Goal and LIBERO-Para. Drop denotes the absolute decrease in success rate.

$T$ . Fig. 4 (bottom) illustrates the computation of  $S_T$ . Lower values of  $S_T(T_O, T_P)$  indicate greater structural divergence, such as word-order changes or reorganization of modification relations.

## 4.3 PRIDE Score

Robustly assessing paraphrased robotic manipulation instructions requires considering both (i) whether task-critical action/object keywords are preserved ( $S_K$ ) and (ii) how much the imperative structure is altered ( $S_T$ ). Accordingly, we define Paraphrase Distance (PD) by combining  $S_K$  and  $S_T$  to quantify the overall deviation between an original robotic instruction and its paraphrase:

$$\text{PD} = 1 - \left( \alpha S_K(O, P) + (1 - \alpha) S_T(T_O, T_P) \right), \quad (3)$$

where  $\alpha \in [0, 1]$  controls the relative contribution of keyword and structural similarity ( $\alpha = 0.5$  by default). Higher PD indicates greater semantic and structural deviation.

$$\text{PRIDE} = \begin{cases} \text{PD}, & \text{success} \\ 0, & \text{failure.} \end{cases} \quad (4)$$

This score complements binary success metrics by distinguishing whether a VLA model can succeed under paraphrased instructions that exhibit larger semantic and structural deviations.

## 5 Experiment

### 5.1 Setup

We evaluate seven model configurations (0.6B–7.5B) spanning four architecture families: parallel decoding with action chunking (OpenVLA-OFT), VLMs with a flow-matching action expert ( $\pi_{0.5}$ , Xiaomi-Robotics-0), soft-prompted cross-embodiment (X-VLA), and bridge-based adaptation (VLA-Adapter). Within the same architecture, we include controlled comparisons on fine-tuning

Method	SR	PRIDE	Overestimation (%)
VLA-Adapter	46.3	36.1	<b>22.0</b>
$\pi_{0.5}$ (expert-only)	39.1	32.0	<b>18.2</b>
X-VLA	62.1	52.7	<b>15.1</b>
OpenVLA-OFT <sub>mixed</sub>	63.7	56.3	<b>11.6</b>
OpenVLA-OFT <sub>goal</sub>	64.7	58.8	<b>9.1</b>
Xiaomi-Robotics-0	76.0	69.2	<b>8.9</b>
$\pi_{0.5}$	71.4	65.4	<b>8.4</b>

Table 3: SR and PRIDE scores on LIBERO-Para, sorted by overestimation. Overestimation is computed as  $(SR - PRIDE) / SR$ , indicating how much uniform success rate overstates a model’s paraphrase robustness.

data scope (OFT<sub>goal</sub> vs. OFT<sub>mixed</sub>) and VLM training strategy ( $\pi_{0.5}$  full vs. expert-only). Full specifications are in Appendix C.1.

## 5.2 Results

**Success Rate Comparison.** Tab. 2 compares success rates between LIBERO-Goal and LIBERO-Para. All models exhibit consistent performance degradation ranging from 22.8 pp to 51.9 pp, indicating that the effect is not architecture-specific but pervasive across models. Even the top-performing models on LIBERO-Goal (Xiaomi-Robotics-0: 98.8%, VLA-Adapter: 98.2%) suffer drops of 22.8 pp and 51.9 pp under paraphrasing, respectively, with VLA-Adapter losing nearly half of its performance.

**PRIDE Reveals Hidden Severity.** Uniform SR treats all paraphrases equally, assigning the same reward to easy and difficult variations, and thus cannot distinguish success limited to easy paraphrases from success that generalizes to harder ones. PRIDE mitigates this limitation by weighting rewards by difficulty. Tab. 3 re-evaluates the same results under PRIDE. VLA-Adapter (22.0%) and  $\pi_{0.5}$  expert-only (18.2%) show large drops relative to SR, indicating success mainly on easy paraphrases and systematic failures on harder variations. In contrast,  $\pi_{0.5}$  (8.4%) and Xiaomi-Robotics-0 (8.9%) exhibit lower overestimation, showing more uniform robustness.

Fig. 5 and Fig. 6 confirm these trends at cell level: degradation intensifies along both axes, with the sharpest drops when object paraphrasing combines with indirect actions. Notably, the gap between object-preserved rows (None, Addition) and object-paraphrased rows (SP-contextual, SP-habitual) is substantially larger than the action-type gap within the same object condition, suggesting that object-level variation is a stronger driver of failure than

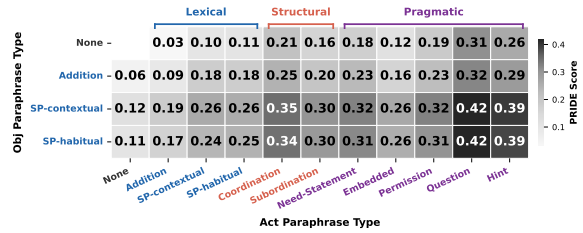


Figure 5: Average PRIDE score per Object  $\times$  Action cell in LIBERO-Para (darker = harder). Scores increase along both axes, with the most indirect action types (Question, Hint) combined with object paraphrasing reaching the highest (SP-habitual  $\times$  Question: 0.42).

action indirectness. We investigate this asymmetry and its underlying causes in Sec. 6.2–6.3, after first examining whether architecture or training choices mitigate the overall degradation (Sec. 6.1).

## 6 Analysis

### 6.1 Finding 1: Paraphrase Fragility Persists Across Architectures, Data Scales, and Fine-tuning Strategies

Before analyzing where and how failures occur in Sec. 6.2 and 6.3, we examine whether paraphrase fragility can be attributed to specific factors by varying architecture family, training data scope, and VLM fine-tuning strategy.

**Architecture Diversity.** Across seven configurations spanning four architecture families (OpenVLA-OFT,  $\pi_{0.5}$ /Xiaomi-Robotics-0, X-VLA, VLA-Adapter), all models show substantial success rate drops under paraphrasing, ranging from 22.8 pp to 51.9 pp (Tab. 2). The 7.5B OpenVLA-OFT shows PRIDE scores comparable to the 0.9B X-VLA. All models exhibit PRIDE overestimation of 8.4–22.0% (Tab. 3). Overall, VLAs consistently experience significant performance degradation under paraphrased instructions, regardless of architecture or scale.

**Data Scope.** OpenVLA-OFT<sub>mixed</sub> expands task-level data diversity by 4 $\times$  compared to OpenVLA-OFT<sub>goal</sub> within the same architecture and simulator. However, both models exhibit similar success rate drops on LIBERO-Para (32.4 pp vs. 33.2 pp), suggesting that increasing task diversity through additional training samples does not improve robustness to linguistic variation in learned tasks.

**VLM Training Strategy.** We compare the standard  $\pi_{0.5}$  model (jointly fine-tuning the VLM and Action Expert) with a variant that freezes the VLM

Obj Paraphrase Type	Act Paraphrase Type										
	None	Addition	SP-contextual	SP-habitual	Coordination	Subordination	Need	Embedded	Permission	Question	Hint
None	90.8	90.3	91.1	80.2	84.8	81.4	87.7	80.6	65.1	68.7	
Addition	93.6	86.0	78.9	81.0	71.7	77.3	75.1	79.2	75.3	62.8	62.7
SP-contextual	70.3	49.5	41.5	45.4	37.1	44.8	37.7	43.1	34.2	31.5	31.6
SP-habitual	71.8	53.8	48.0	48.5	40.3	43.9	40.2	46.8	39.2	33.2	30.4

Figure 6: Model-average success rate per Object  $\times$  Action cell. Object-paraphrased rows drop sharply compared to object-preserved rows, reaching 30.4% at SP-habitual  $\times$  Hint.

of the base VLA and fine-tunes only the Action Expert. The frozen-VLM variant shows substantially lower performance on LIBERO-Goal (97.6  $\rightarrow$  78.6; Tab. 2) and does not exhibit improved robustness on LIBERO-Para (SR: 39.1, PRIDE: 32.0; Tab. 3). Although the jointly fine-tuned model achieves higher success rates on LIBERO-Para (71.4 vs. 39.1), both variants still show substantial drops under paraphrasing. This suggests that joint adaptation of the VLM and Action Expert is essential for downstream performance, while fine-tuning on limited demonstrations may degrade pretrained semantics, causing paraphrase vulnerability. Taken together, paraphrase fragility persists across all three factors. This indicates that the robustness gap cannot be explained solely by architecture, data scope, or fine-tuning strategy, but points to a deeper challenge. *Which linguistic variations, then, are most responsible for these failures?*

## 6.2 Finding 2: Object Grounding Emerges as a Primary Bottleneck

Sec. 6.1 shows that paraphrase fragility persists regardless of architecture, data scope, or fine-tuning strategy. We next examine where this degradation concentrates. Our analysis reveals an asymmetry: object-level variation emerges as the dominant source of failure, while action indirectness introduces additional degradation.

Fig. 7 compares success rates between object-preserved and object-paraphrased instructions across models. When the object is paraphrased—even through common synonyms such as replacing *stove* with *range*—performance drops by 19.8 pp ( $\pi_{0.5}$  expert-only) to 51.0 pp (OpenVLA-OFT<sub>mixed</sub>) across models. This gap appears consistently across architectures, suggesting that current VLAs rely more on surface-level keyword matching than on semantic understanding of ob-

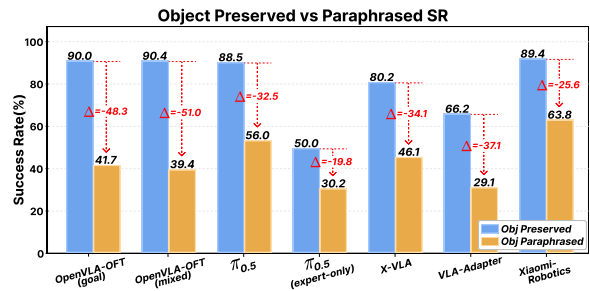


Figure 7: Success rate comparison between object-preserved (None, Addition) and object-paraphrased (SP-contextual, SP-habitual) instructions. All models show substantial drops, from 19.8 pp ( $\pi_{0.5}$  expert-only) to 51.0 pp (OpenVLA-OFT<sub>mixed</sub>).  $\Delta$  annotated per pair.

jects. Notably, OpenVLA-OFT<sub>mixed</sub>, trained with four times more tasks, exhibits nearly the same gap as OpenVLA-OFT<sub>goal</sub> (51.0 pp vs. 48.3 pp; Fig. 7), indicating that task diversity and object-paraphrase robustness are decoupled. PRIDE  $\alpha$  sweep experiments further confirm that keyword-level lexical variation around object references drives most of the degradation, compared to syntactic restructuring (Appendix D.2). In addition, action indirectness introduces a stepwise performance decline: as instructions become less explicit, success rates drop from 82.7% (None) to around 48% (Question, Hint) (see Appendix D.2 for the full action-axis breakdown).

This asymmetry reflects structural properties of tabletop manipulation. The action space is restricted to a small set of motor primitives (e.g., pick, place, push, open), and each object typically supports only a few feasible actions (e.g., *stove*  $\rightarrow$  turn on), allowing models to converge to the correct primitive even under varied phrasing. In contrast, the object space is much larger and lexically open-ended, concentrating combinatorial complexity on object references. This vulnerability may be amplified by current VLA training data, where

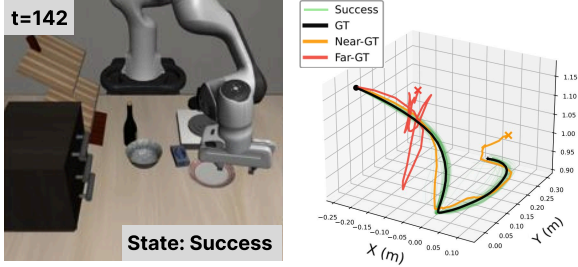


Figure 8: (Left) LIBERO scene for Task 2: Push the plate to the front of the stove. (Right) 3D end-effector trajectories under a paraphrased instruction ( $\pi_{0.5}$ ). Green: successful episodes; black: their mean (GT); orange: Near-GT failure (tracks GT but fails); red: Far-GT failure (diverges early).

objects are often referred to by a single canonical name (Fig. 12), making grounding sensitive even to simple synonym substitutions. These observations suggest that the primary bottleneck in paraphrase robustness lies in object grounding, with action indirectness introducing additional degradation.

Having identified the dominant factor behind these failures, we next ask: *do these failures arise during execution of the correct task, or do models generate different trajectories from the outset?*

### 6.3 Finding 3: Failures Are Predominantly Planning-Level, Not Execution-Level

Sec. 6.2 identified object grounding as the primary bottleneck, with action indirectness introducing additional degradation. To determine whether failures arise during execution of the correct task or from generating entirely different trajectories from the outset, we classify failures based on trajectory similarity to successful executions. For each task, we define the mean successful trajectory as pseudo ground-truth (hereafter GT) and compute the Dynamic Time Warping (DTW) distance (Sakoe and Chiba, 1978) between each failure trajectory and the GT. Because LIBERO-Goal training data follows a fixed trajectory with minimal path variation, the mean success trajectory serves as a reliable pseudo GT. Failures within a threshold  $\tau$  (the maximum DTW distance among successful episodes) are categorized as **Near-GT** (execution-level), indicating correct task execution but failure due to minor motor control errors. Failures exceeding  $\tau$  are categorized as **Far-GT** (planning-level), indicating fundamentally different trajectories and thus failure in task identification. As shown in Fig. 8, Near-GT trajectories remain close to suc-

Model	Success Rate	Failure		
		Near-GT	Far-GT	Far-GT(%)
OpenVLA-OFT <sub>goal</sub>	64.7	1.6	33.7	<b>95.5</b>
Xiaomi-Robotics-0	76.0	1.8	22.2	<b>92.5</b>
VLA-Adapter	46.3	4.2	49.5	<b>92.2</b>
$\pi_{0.5}$	71.4	2.4	26.2	<b>91.6</b>
OpenVLA-OFT <sub>mixed</sub>	63.7	3.3	33.0	<b>90.9</b>
X-VLA	62.1	5.2	32.7	<b>86.3</b>
$\pi_{0.5}$ (expert-only)	39.1	12.5	48.4	<b>79.5</b>

Table 4: Failure classification on LIBERO-Para (by Far-GT (%)). Near-GT: execution-level failure near GT trajectory. Far-GT: planning-level failure from GT. Across models, 79.5–95.5% of failures are planning-level.

cessful ones, whereas Far-GT trajectories diverge substantially. Additional methodological details are provided in Appendix D.3.

Tab. 4 summarizes the classification results. Across models, 79.5%–95.5% of failures are Far-GT, while Near-GT cases account for less than 5% in most models. This indicates that under paraphrased instructions, models rarely fail along the correct trajectory but instead generate different trajectories from the outset. The only exception is  $\pi_{0.5}$  expert-only (Near-GT: 12.5%), where the frozen VLM may identify the task correctly but the non-adapted Action Expert fails to execute it precisely, consistent with the VLM training strategy analysis in Sec. 6.1. These findings align with Sec. 6.2: when object grounding fails, the model plans actions toward incorrect targets, producing trajectories that diverge from the GT. The dominant failure mode lies in task identification rather than motor control, suggesting that improving paraphrase robustness should focus on instruction semantic-to-task mapping rather than action-execution control.

## 7 Conclusion

This work investigates paraphrase robustness in modern VLA models using LIBERO-Para, a controlled benchmark that independently varies action and object expressions, and PRIDE, a metric for fine-grained robustness assessment. We find that paraphrase fragility persists across architectures, scales, and fine-tuning strategies, with object-level lexical variation as the dominant source of degradation and 80–96% of failures arising from planning-level trajectory divergence rather than execution errors. These results reveal a fundamental limitation: current VLA models struggle to map diverse linguistic instructions to correct task identification, relying on surface-level matching instead of ro-



bust object grounding. These findings suggest that improving robustness to paraphrased instructions requires prioritizing instruction-to-task identification over low-level control refinement, with object grounding as a key direction.

## Limitations

This study evaluates VLA models within the LIBERO simulation environment. As simulations differ from real-world settings in rendering fidelity, physics modeling, and sensor noise, further validation is required to determine whether the observed vulnerabilities in paraphrase robustness persist on physical robotic platforms. In addition, our paraphrase design considers a single variation type along each axis at a time. In natural language use, however, multiple variations may co-occur—for example, synonym substitution combined with adverb insertion, or structural reorganization coupled with indirect speech acts. Such compound variations can introduce more complex linguistic shifts and may pose greater challenges to VLA models. While this work focuses on isolating and analyzing the effects of individual variation types, the analysis of compound paraphrase variations is deferred to future work. Also, we do not investigate paraphrase-based data augmentation as a mitigation strategy, since augmentation using LLM-generated paraphrases could introduce distributional overlap with the benchmark, which may confound the evaluation.

## References

- Anthropic. 2025. System card: Claude opus 4 & claude sonnet 4. Anthropic system card.
- Nikolaus Augsten and Michael H. Böhlen. 2013. *Similarity Joins in Relational Database Systems*. Synthesis Lectures on Data Management. Morgan & Claypool Publishers.
- Shuai Bai, Qwen Team, and 1 others. 2025. [Qwen3-v1 technical report](#). *arXiv preprint arXiv:2511.21631*.
- Satanjeev Banerjee and Alon Lavie. 2005. Meteor: An automatic metric for mt evaluation with improved correlation with human judgments. In *Proceedings of the acl workshop on intrinsic and extrinsic evaluation measures for machine translation and/or summarization*, pages 65–72.
- Kevin Black, Noah Brown, Danny Driess, Adnan Esmael, Michael Equi, Chelsea Finn, Niccolo Fusai, Lachy Groom, Karol Hausman, Brian Ichter, Szymon Jakubczak, Tim Jones, Liyiming Ke, Sergey Levine, Adrian Li-Bell, Mohith Mothukuri, Suraj Nair, Karl Pertsch, Lucy Xiaoyang Shi, and 6 others. 2024.  [\$\pi\_0\$ : A vision-language-action flow model for general robot control](#). *arXiv preprint arXiv:2410.24164*.
- Qingwen Bu, Jisong Cai, Li Chen, Xiuqi Cui, Yan Ding, Siyuan Feng, Shenyuan Gao, Xindong He, Xuan Hu, Xu Huang, and 1 others. 2025. Agibot world colosseum: A large-scale manipulation platform for scalable and intelligent embodied systems. *arXiv preprint arXiv:2503.06669*.
- Rui Cai, Jun Guo, Xinze He, Piaopiao Jin, Jie Li, Bingxuan Lin, Futeng Liu, Wei Liu, Fei Ma, Kun Ma, and 1 others. 2026. [Xiaomi-robotics-0: An open-sourced vision-language-action model with real-time execution](#). *arXiv preprint arXiv:2602.12684*.
- Gheorghe Comanici, Eric Bieber, Mike Schaeckermann, Ice Pasupat, Noveen Sachdeva, Inderjit Dhillon, Marcel Blistein, Ori Ram, Dan Zhang, Evan Rosen, and 1 others. 2025. Gemini 2.5: Pushing the frontier with advanced reasoning, multimodality, long context, and next generation agentic capabilities. *arXiv preprint arXiv:2507.06261*.
- Susan Ervin-Tripp. 1976. [Is Sybil there? The structure of some American English directives](#). *Language in Society*, 5(1):25–66.
- Senyu Fei, Siyin Wang, Junhao Shi, Zihao Dai, Jikun Cai, Pengfang Qian, Li Ji, Xinzhe He, Shiduo Zhang, Zhaoye Fei, Jinlan Fu, Jingjing Gong, and Xipeng Qiu. 2025. [Libero-plus: In-depth robustness analysis of vision-language-action models](#). *arXiv preprint arXiv:2510.13626*.
- Alvan R Feinstein and Domenic V Cicchetti. 1990. High agreement but low kappa: I. the problems of two paradoxes. *Journal of clinical epidemiology*, 43(6):543–549.
- Zipeng Fu, Tony Z. Zhao, and Chelsea Finn. 2024. [Mobile ALOHA: Learning bimanual mobile manipulation with low-cost whole-body teleoperation](#). *arXiv preprint arXiv:2401.02117*.
- Kilem Li Gwet. 2008. Computing inter-rater reliability and its variance in the presence of high agreement. *British Journal of Mathematical and Statistical Psychology*, 61(1):29–48.
- Yuchen Hou and Lin Zhao. 2026. [Langgap: Diagnosing and closing the language gap in vision-language-action models](#). *arXiv preprint arXiv:2603.00592*.
- Siddharth Karamcheti, Suraj Nair, William Brown, Abhiram Maddukuri, Takuma Osa, Chelsea Finn, Percy Liang, Sergey Levine, Ted Xiao, and 1 others. 2024. [Prismatic vlms: Investigating the design space of visually-conditioned language models](#). *arXiv preprint arXiv:2402.07865*.
- Alexander Khazatsky, Karl Pertsch, Suraj Nair, Ashwin Balakrishna, Sudeep Dasari, Siddharth Karamcheti, Soroush Nasiriany, Mohan Kumar Srirama,

- Lawrence Yunliang Chen, Kirsty Ellis, and 1 others. 2024. Droid: A large-scale in-the-wild robot manipulation dataset. *arXiv preprint arXiv:2403.12945*.
- Moo Jin Kim, Chelsea Finn, and Percy Liang. 2025. [Fine-tuning vision-language-action models: Optimizing speed and success](#). *arXiv preprint arXiv:2502.19645*.
- Moo Jin Kim, Karl Pertsch, Siddharth Karamcheti, Ted Xiao, Ashwin Balakrishna, Suraj Nair, Rafael Rafailov, Ethan Foster, Grace Lam, Pannag Sanketi, Quan Vuong, Thomas Kollar, Benjamin Burchfiel, Russ Tedrake, Dorsa Sadigh, Sergey Levine, Percy Liang, and Chelsea Finn. 2024. [Openvla: An open-source vision-language-action model](#). *arXiv preprint arXiv:2406.09246*.
- Venelin Kovatchev, M. Antònia Martí, and Maria Salamó. 2018. [ETPC - a paraphrase identification corpus annotated with extended paraphrase typology and negation](#). In *Proceedings of the Eleventh International Conference on Language Resources and Evaluation (LREC 2018)*, Miyazaki, Japan. European Language Resources Association (ELRA).
- Bo Liu, Yifeng Zhu, Chongkai Gao, Yihao Feng, Qiang Liu, Yuke Zhu, and Peter Stone. 2023. [Libero: Benchmarking knowledge transfer for lifelong robot learning](#). In *Advances in Neural Information Processing Systems (NeurIPS), Datasets and Benchmarks Track*, volume 36, pages 44776–44791.
- Ilya Loshchilov and Frank Hutter. 2017. Decoupled weight decay regularization. *arXiv preprint arXiv:1711.05101*.
- Oier Mees, Lukas Hermann, Erick Rosete-Beas, and Wolfram Burgard. 2021. [CALVIN: A benchmark for language-conditioned policy learning for long-horizon robot manipulation tasks](#). *arXiv preprint arXiv:2112.03227*.
- George A Miller. 1995. Wordnet: a lexical database for english. *Communications of the ACM*, 38(11):39–41.
- OpenAI. 2023. Gpt-4 technical report. *arXiv preprint arXiv:2303.08774*.
- Abby O’Neill, Abdul Rehman, Abhiram Maddukuri, Abhishek Gupta, Abhishek Padalkar, Abraham Lee, Acorn Pooley, Agrim Gupta, Ajay Mandekar, Ajinkya Jain, and 1 others. 2024. Open x-embodiment: Robotic learning datasets and rt-x models: Open x-embodiment collaboration 0. In *2024 IEEE International Conference on Robotics and Automation (ICRA)*, pages 6892–6903. IEEE.
- Kishore Papineni, Salim Roukos, Todd Ward, and Wei-Jing Zhu. 2002. Bleu: a method for automatic evaluation of machine translation. In *Proceedings of the 40th annual meeting of the Association for Computational Linguistics*, pages 311–318.
- Physical Intelligence, Kevin Black, Noah Brown, James Darpinian, Karan Dhabalia, Danny Driess, Adnan Esmail, Michael Equi, Chelsea Finn, Niccolo Fusai, Manuel Y. Galliker, Dibya Ghosh, Lachy Groom, Karol Hausman, Brian Ichter, Szymon Jakubczak, Tim Jones, Liyiming Ke, Devin LeBlanc, and 18 others. 2025.  [\$\pi\_{0.5}\$ : a vision-language-action model with open-world generalization](#). *arXiv preprint arXiv:2504.16054*.
- Nils Reimers and Iryna Gurevych. 2019. Sentence-bert: Sentence embeddings using siamese bert-networks. In *Proceedings of the 2019 Conference on Empirical Methods in Natural Language Processing and the 9th International Joint Conference on Natural Language Processing (EMNLP-IJCNLP)*, pages 3982–3992.
- Hiroaki Sakoe and Seibi Chiba. 1978. [Dynamic programming algorithm optimization for spoken word recognition](#). *IEEE Transactions on Acoustics, Speech, and Signal Processing*, 26(1):43–49.
- Stan Salvador and Philip Chan. 2007. Toward accurate dynamic time warping in linear time and space. *Intelligent data analysis*, 11(5):561–580.
- Andreas Steiner, André Susano Pinto, Michael Tschanen, Daniel Keysers, Xiao Wang, Yonatan Bitton, Alexey Gritsenko, Matthias Minderer, Anthony Sherbondy, Shangbang Long, Siyang Qin, Reeve Ingle, Emanuele Bugliarello, Sahar Kazemzadeh, Thomas Mesnard, Ibrahim Alabdulmohsin, Lucas Beyer, and Xiaohua Zhai. 2024. [Paligemma 2: A family of versatile vlms for transfer](#). *arXiv preprint arXiv:2412.03555*.
- Qwen Team. 2024. [Qwen2.5 technical report](#). *arXiv preprint arXiv:2412.15115*.
- Hugo Touvron, Louis Martin, Kevin Stone, Peter Albert, Amjad Almahairi, Yasmine Babaei, Nikolay Bashlykov, Soumya Batra, Prajjwal Bhargava, Shrubti Bhosale, and 1 others. 2023. [Llama 2: Open foundation and fine-tuned chat models](#). *arXiv preprint arXiv:2307.09288*.
- Guodong Wang, Chenkai Zhang, Qingjie Liu, Jinjin Zhang, Jiancheng Cai, Junjie Liu, and Xinmin Liu. 2026. [Libero-x: Robustness litmus for vision-language-action models](#). *arXiv preprint arXiv:2602.06556*.
- Yihao Wang, Pengxiang Ding, Lingxiao Li, Can Cui, Zirui Ge, Xinyang Tong, Wenxuan Song, Han Zhao, Wei Zhao, Pengxu Hou, and 1 others. 2025. [Vla-adapter: An effective paradigm for tiny-scale vision-language-action model](#). *arXiv preprint arXiv:2509.09372*.
- Zhijie Wang, Zhehua Zhou, Jiayang Song, Yuheng Huang, Zhan Shu, and Lei Ma. 2024. [LADEV: A language-driven testing and evaluation platform for vision-language-action models in robotic manipulation](#). *arXiv preprint arXiv:2410.05191*.

- Jimmy Wu, Rika Antonova, Adam Kan, Marion Lepert, Andy Zeng, Shuran Song, Jeannette Bohg, Szymon Rusinkiewicz, and Thomas Funkhouser. 2023. [Tidybot: Personalized robot assistance with large language models](#). *arXiv preprint arXiv:2305.05658*.
- Kun Wu, Chengkai Hou, Jiaming Liu, Zhengping Che, Xiaozhu Ju, Zhuqin Yang, Meng Li, Yinuo Zhao, Zhiyuan Xu, Guang Yang, and 1 others. 2024. Robomind: Benchmark on multi-embodiment intelligence normative data for robot manipulation. *arXiv preprint arXiv:2412.13877*.
- Bin Xiao, Haiping Wu, Wei Xu, Jifeng Dai, Xiaowei Hu, Yichen Lu, Michael Zeng, and 1 others. 2024. [Florence-2: Advancing a unified representation for a variety of vision tasks](#). In *Proceedings of the IEEE/CVF Conference on Computer Vision and Pattern Recognition (CVPR)*, pages 4810–4821.
- Yajat Yadav, Zhiyuan Zhou, Andrew Wagenmaker, Karl Pertsch, and Sergey Levine. 2025. [Robust finetuning of vision-language-action robot policies via parameter merging](#). *arXiv preprint arXiv:2512.08333*.
- Tianyi Zhang, Varsha Kishore, Felix Wu, Kilian Q Weinberger, and Yoav Artzi. 2019. Bertscore: Evaluating text generation with bert. *arXiv preprint arXiv:1904.09675*.
- Jinliang Zheng, Jianxiong Li, Zhihao Wang, Dongxiu Liu, Xirui Kang, Yuchun Feng, Yanan Zheng, Jiayin Zou, Yilun Chen, Jia Zeng, and 1 others. 2025. [Xvla: Soft-prompted transformer as scalable cross-embodiment vision-language-action model](#). *arXiv preprint arXiv:2510.10274*.
- Xueyang Zhou, Yangming Xu, Guiyao Tie, Yongchao Chen, Guowen Zhang, Duanfeng Chu, Pan Zhou, and Lichao Sun. 2025. [LIBERO-PRO: Towards robust and fair evaluation of vision-language-action models beyond memorization](#). *arXiv preprint arXiv:2510.03827*.
- Brianna Zitkovich and 1 others. 2023. [RT-2: Vision-language-action models transfer web knowledge to robotic control](#). In *Proceedings of The 7th Conference on Robot Learning (CoRL)*, volume 229 of *Proceedings of Machine Learning Research*, pages 2165–2183.

# APPENDIX

## Contents

<b>A</b>	<b>LIBERO-Para: A Controlled VLA Benchmark for Paraphrase Robustness</b>	<b>13</b>
A.1	Excluded Types from Extended Paraphrase Typology . . . . .	13
A.2	Excluded Type from Directive Types . . . . .	14
A.3	Paraphrase Dataset Generation . . . . .	14
A.4	Statistics of LIBERO-Para . . . . .	15
A.5	Human Evaluation . . . . .	15
<b>B</b>	<b>PRIDE: Paraphrase Robustness Index in Robotic Instructional DEviation</b>	<b>16</b>
<b>C</b>	<b>Experiment</b>	<b>17</b>
C.1	Setup . . . . .	17
C.2	Result . . . . .	18
<b>D</b>	<b>Analysis</b>	<b>18</b>
D.1	Finding 1: Paraphrase Fragility Persists Across Architectures, Data Scales, and Fine-tuning Strategies . . . . .	18
D.2	Finding 2: Object Grounding Is the Primary Bottleneck . . . . .	19
D.3	Finding 3: Failures Are Predominantly Planning-Level, Not Execution-Level .	20
<b>E</b>	<b>AI Assistants</b>	<b>22</b>

Category	Type	Source (Year)
Obj-Lexical	same polarity habitual	EPT (2018)
	Same polarity contextual Addition	
Act-Lexical	Same polarity habitual	EPT (2018)
	Same polarity contextual Addition	
Act-Structural	Coordination Subordination	EPT (2018)
Act-Pragmatic	Personal need	Directive Types (1976)
	Question directive	
	Embedded imperative	
	Permission Hint	

Table 5: Selected paraphrase types in LIBERO-Para. Types are derived from Extended Paraphrase Typology (EPT) (Kovatchev et al., 2018) and Directive Types (Ervin-Tripp, 1976).

## A LIBERO-Para: A Controlled VLA Benchmark for Paraphrase Robustness

This appendix details the paraphrase taxonomy adopted in LIBERO-Para and explains the rationale for excluding certain types from the source taxonomies (EPT and Directive Types). Our taxonomy is grounded in the Extended Paraphrase Typology (EPT) (Kovatchev et al., 2018) and the Directive types proposed by Ervin-Tripp (1976). From the 26 atomic paraphrase types in EPT and the six different types in Directive Types, we select 13 types that satisfy the following criteria: (i) applicability to robotic manipulation instructions (i.e., direct imperatives), (ii) preservation of the original meaning, (iii) compliance with visual and spatial constraints, and (iv) grammatical naturalness. All paraphrases are generated under these constraints and are used exclusively for evaluation.

### A.1 Excluded Types from Extended Paraphrase Typology

While EPT provides a broad inventory of paraphrase operations, many types are unsuitable for robotic manipulation instructions under our design constraints. Tab. 6 presents the Extended Paraphrase Typology (EPT), summarizing its high-level categories along with their corresponding atomic types.

**Morphology.** We exclude the entire Morphology category. Inflectional changes may alter object cardinality (e.g., pluralization) or modify temporal interpretation when applied to actions. Modal verb changes can shift intent, introducing semantic drift. Derivational changes alter part-of-speech (e.g., “pick” → “picker”), which violates impera-

Categories	Atomic Type
Morphology	Inflectional changes
	Modal verb changes
	Derivational changes
Lexicon	Spelling changes
	Same polarity substitution (habitual)
	Same polarity substitution (contextual)
	Same polarity substitution (named entities) Change of format
Lexical-syntactic	Opposite polarity substitution (habitual)
	Opposite polarity substitution (contextual)
	Synthetic/analytic substitution
	Converse substitution
Syntax	Diathesis alternation
	Negation switching
	Ellipsis
	Coordination changes
	Subordination and nesting changes
Discourse	Punctuation changes
	Direct/indirect style alternations
	Sentence modality changes
	Syntax/discourse structure changes
Other	Addition/Deletion
	Change of order
	Semantic based
Extremes	Identity
	Non-paraphrase Entailment

Table 6: Extended Paraphrase Typology (EPT) categories and atomic types (Kovatchev et al., 2018).

tive structure or disrupts the intended reference.

**Lexicon.** We retain same polarity substitution (habitual and contextual) and exclude the remaining types. Spelling changes are insufficient to constitute meaningful variation. Same polarity substitution involving named entities is rarely applicable, as robotic instructions predominantly use common nouns and generic verbs. Change of format is often either trivial or difficult to apply while preserving meaning.

**Lexical-syntactic.** We exclude this category in its entirety. Opposite polarity substitution is unnatural for object nouns and leads to awkward or unintended speech acts when applied to actions. Synthetic/analytic substitutions (e.g., “*bow*” ↔ “*round container*”) are unnatural in concise imperatives. Converse substitutions introduce role-swapping constructions that are rarely natural in commands.

**Syntax.** We retain coordination and subordination changes and exclude the remaining types. Diathesis alternation yields passive-like commands, which are unnatural in robotic instructions. Negation switching overlaps with opposite polarity substitutions. Ellipsis introduces ambiguity in short imperatives and overlaps with addition/deletion.

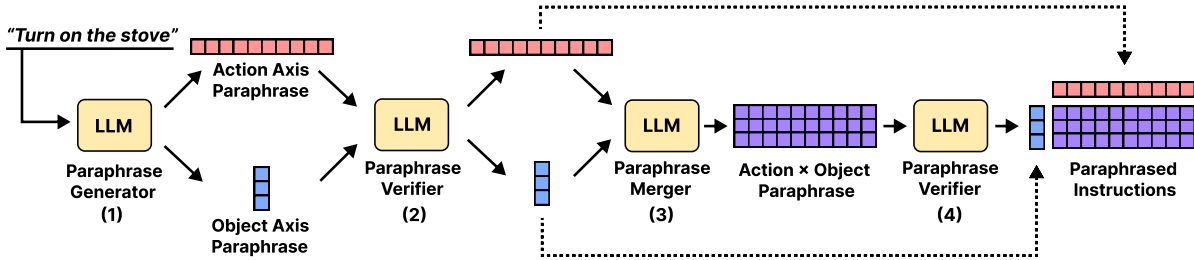


Figure 9: Overview of the LIBERO-Para dataset generation workflow. The process consists of four stages: (1) axis-wise paraphrase generation, (2) verification, (3) merging, and (4) final verification.

Directive Type	Example
Need statements	"I need a match"
Imperatives	"Gimme a match", "a match"
Embedded imperatives	"Could you gimme a match?"
Permission directives	"May I have a match?"
Question directives	"Gotta match?"
Hints	"The matches are all gone"

Table 7: Six directive types from Directive Types (Ervin-Tripp, 1976).

**Discourse.** We exclude this category entirely. Robotic commands are treated as direct imperatives; alternations in style or sentence modality may alter the intended directive force. Syntax/discourse structure changes are overly high-level relative to atomic instructions and hinder controlled evaluation.

**Other.** We retain only addition. Given the brevity of imperative commands, deletion frequently removes essential components or produces ungrammatical outputs. Change of order is often unnatural in short imperatives. Semantic-based types lack a precise definition and are unsuitable for controlled evaluation.

**Extremes.** We exclude this category entirely. Identity involves no transformation. Non-paraphrase violates meaning preservation. Entailment represents an inferential relation rather than a meaning-preserving transformation.

## A.2 Excluded Type from Directive Types

Ervin-Tripp proposed a directive taxonomy that categorizes Directive Types into six types (Ervin-Tripp, 1976), as summarized in Tab. 7. Among these, we select five types for the Action-Pragmatic axis: need statements, embedded imperatives, permission directives, question directives, and hints.

**Imperatives.** We exclude the imperative type from our paraphrase taxonomy. Since imperatives (e.g., "Pick up the bowl") represent the canonical form of robotic manipulation instructions, they

serve as the original instruction rather than a paraphrase variant. In our benchmark design, this type corresponds to the baseline condition (Action axis: None) against which other pragmatic variations are compared.

## A.3 Paraphrase Dataset Generation

This section describes the paraphrase dataset generation process using LLMs. As illustrated in Fig. 9, our workflow consists of four stages: (1) axis-wise paraphrase generation, (2) paraphrase verification, (3) axis merging, and (4) final verification.

**Axis-wise Paraphrase Generation** Given an original instruction, a paraphrase generator (LLM) independently produces paraphrases along the action axis (10 types) and the object axis (3 types). Each generated paraphrase is filtered by a paraphrase verifier (LLM) to ensure meaning preservation and grammatical naturalness.

**Paraphrase Merging** Verified action-axis and object-axis paraphrases modify independent components of the instruction and can therefore be combined. If  $n$  action paraphrases and  $m$  object paraphrases pass verification, up to  $n \times m$  merged paraphrases are possible. Merged paraphrases are further validated by the verifier (LLM) before inclusion in the dataset.

**Design Principles** Rather than prompting a single LLM to generate all paraphrase types jointly, we adopt an axis-wise generation and merging strategy. This modular design assigns a single role to each LLM (generator, merger, and verifier), reducing task complexity and improving generation reliability. All LLM calls use Gemini 2.5 Pro. Detailed prompts used at each stage are provided at the end of the paper for readability, and are illustrated in Figs. 20 to 28.

Object	None	Act-Lexical			Act-Structural		Act-Pragmatic					Total
		add	ctx	hab	coord	subord	need	embed	perm	quest	hint	
None	–	100	79	74	98	75	93	93	83	87	88	870
Addition	98	100	100	100	100	100	100	99	99	99	100	1,095
Contextual	87	100	100	100	100	99	100	100	100	94	96	1,076
Habitual	74	100	98	100	97	94	100	95	100	95	98	1,051
<b>Total</b>	259	400	377	374	395	368	393	387	382	375	382	<b>4,092</b>

**Abbreviations:** add = addition, ctx = same\_polarity\_contextual, hab = same\_polarity\_habitual, coord = coordination, subord = subordination, need = need\_statement, embed = embedded\_imperative, perm = permission\_directive, quest = question\_directive.

Table 8: LIBERO-Para dataset statistics. Each cell shows the number of paraphrased instructions for the corresponding Object (row) and Action (column) variation type combination. “None” indicates no variation on that axis.

Original Instruction	Count
<i>Put the wine bottle on top of the cabinet</i>	423
<i>Open the middle drawer of the cabinet</i>	416
<i>Turn on the stove</i>	414
<i>Put the wine bottle on the rack</i>	413
<i>Put the cream cheese in the bowl</i>	411
<i>Open the top drawer and put the bowl inside</i>	410
<i>Put the bowl on top of the cabinet</i>	410
<i>Push the plate to the front of the stove</i>	406
<i>Put the bowl on the stove</i>	403
<i>Put the bowl on the plate</i>	386
<b>Total</b>	<b>4,092</b>

Table 9: Number of paraphrased instructions per original instruction in LIBERO-Para.

#### A.4 Statistics of LIBERO-Para

LIBERO-Para consists of 4,092 paraphrases generated from 10 original LIBERO-Goal instructions, selected from the four LIBERO task types (Spatial, Object, Goal, and Long) where linguistic understanding is essential for successful execution.

The dataset is organized along two axes: an Object axis with three lexical types, and an Action axis with ten types (three lexical, two structural, and five pragmatic). This two-axis design yields 43 distinct paraphrase type combinations: three Object-only, ten Action-only, and thirty compositional types ( $3 \times 10$ ).

Tab. 8 reports the number of paraphrases for each Object  $\times$  Action combination. The dataset includes 259 Object-only paraphrases (Action = None), 870 Action-only paraphrases (Object = None), and 2,963 compositional paraphrases. To facilitate diverse analyses, samples are distributed approximately uniformly across cells, with around 100 paraphrases per cell.

To examine how each component of PRIDE contributes to paraphrase difficulty, Figs. 10 and 11 present the average keyword distance ( $1 - S_K$ ) and structural distance ( $1 - S_T$ ), respectively, which correspond to isolating each term in the PD formula-

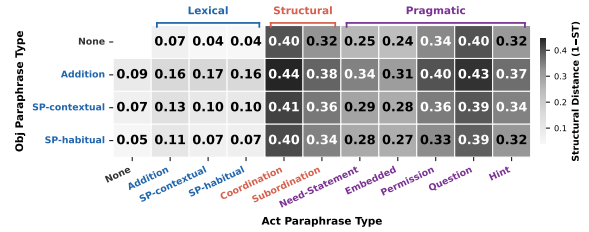


Figure 10: Average Structural Distance ( $1 - S_T$ ) per Object  $\times$  Action cell. This component reflects syntactic divergence only (SK weight = 0.0, ST weight = 1.0 in PRIDE). Unlike keyword distance, structural distance is dominated by action paraphrase type rather than object substitution: Coordination and Subordination columns uniformly score above 0.28 across all rows, while lexical action types remain below 0.17. This confirms that structural rewriting primarily originates from act-level transformations.

tion (Eq. 3). Keyword distance is primarily driven by the Object axis: contextual and habitual substitutions yield high distances (0.41–0.45) due to synonym replacement, while rows without object paraphrasing remain near zero. Structural distance, in contrast, is dominated by the Action axis: coordination and subordination columns consistently score above 0.28 regardless of object type, whereas lexical action types stay below 0.17. This decomposition confirms that the two PRIDE components capture complementary sources of difficulty—lexical divergence from object paraphrasing and syntactic divergence from action paraphrasing.

Finally, Tab. 9 reports the number of paraphrases per original instruction. Each instruction yields 386–423 paraphrases, indicating a balanced distribution.

#### A.5 Human Evaluation

To verify the semantic validity of LIBERO-Para, we conducted a human evaluation on a randomly sampled 5% subset (205 samples) of the full bench-

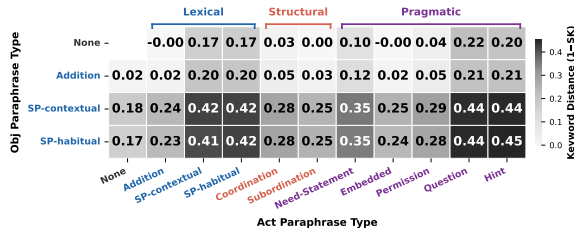


Figure 11: Average Keyword Distance ( $1 - S_K$ ) per Object  $\times$  Action cell. This component reflects lexical divergence only (SK weight = 1.0, ST weight = 0.0 in PRIDE). Scores are driven primarily by object paraphrasing: rows with SP-contextual or SP-habitual substitutions consistently score higher regardless of action type. Among action types, Question and Hint columns show the highest values, with SP-habitual  $\times$  Hint reaching 0.45.

mark. Fifteen annotators independently judged whether each original–paraphrase pair would elicit the same successful behavior in the given scene, using a binary Yes/No decision.

**Inter-Annotator Agreement.** We report Gwet’s AC1 (Gwet, 2008) as the inter-annotator agreement (IAA) metric. We chose AC1 over Cohen’s or Fleiss’  $\kappa$  because our labels are heavily skewed toward the positive class, a setting in which  $\kappa$  is known to be substantially deflated despite high observed agreement (Feinstein and Cicchetti, 1990). On our 15-annotator evaluation, Gwet’s AC1 is **0.854**, indicating strong agreement.

**Consensus Statistics.** Under a majority-vote criterion ( $\geq 8/15$  annotators marking Yes), 204 out of 205 samples (99.51%) were judged as meaning-preserving. Under a stricter threshold requiring  $\geq 12/15$  agreement (80%), 183 out of 205 samples (89.27%) passed. Across all 205 samples, annotators selected Yes at an average rate of 14.13/15 (94.18%), further supporting high item-level consensus.

**Error Analysis.** We examined the 22 samples that failed the stricter criterion and found that disagreement was concentrated in paraphrases where the original imperative form was transformed into suggestive, declarative, or indirect speech-act forms. This indicates that disagreement primarily arose from differences in annotator interpretation of speech-act form rather than semantic distortion of the paraphrase itself. At the same time, such cases confirm that the benchmark includes pragmatically challenging linguistic reformulations that

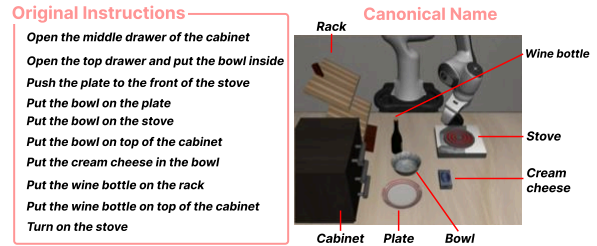


Figure 12: LIBERO-Goal task instructions (left) and corresponding scene with canonical object names (right). Each object is referred to by a single unique keyword throughout all instructions (e.g., *stove*, *bowl*, *rack*), with no lexical variation across tasks.

go beyond simple lexical substitution.

**Annotation Protocol.** Each annotator received an Excel spreadsheet containing 205 randomly sampled original–paraphrase pairs. They were instructed to mark 0 if the paraphrased instruction would elicit the same successful behavior as the original instruction in the given VLA scene (LIBERO-Goal initial scene), and X otherwise. The 15 annotators included participants with varying levels of familiarity with robotic manipulation tasks, ranging from domain-familiar researchers to non-expert volunteers. All annotators were informed that their responses would be used for research purposes.

## B PRIDE: Paraphrase Robustness Index in Robotic Instructional DEviation

**Motivation.** General-purpose NLP distance metrics such as BERTScore (Zhang et al., 2019), BLEU (Papineni et al., 2002), and METEOR (Banerjee and Lavie, 2005) are designed to measure surface-level or semantic similarity between text pairs, without considering how linguistic changes affect downstream task execution. In grounded robotic instruction following, however, not all lexical changes are equally disruptive: replacing a task-critical object noun (e.g., “stove”  $\rightarrow$  “range”) directly impacts visual grounding and action selection, whereas syntactic additions (e.g., prepending “carefully”) leave the core command intact. PRIDE is designed to reflect this asymmetry by decomposing paraphrase distance into two robot-relevant axes: keyword divergence ( $S_K$ ), which captures whether task-critical referents are preserved, and structural divergence ( $S_T$ ), which measures how far the utterance departs from the imperative form that VLA models are



Original	Paraphrase	Type	SR(%)	PRIDE	$1 - S_K$	$1 - S_T$	1-BERT	1-BLEU	1-METEOR
Put the cream cheese in the bowl	“carefully put the cream cheese in the bowl”	addition(act)	90.8	0.03	0.00	0.07	0.14	0.16	0.02
	“put the cheese spread in the vessel”	SP-contextual(obj)	70.3	0.35	0.27	0.43	0.12	0.80	0.36
	“Is the spread supposed to go in the container?”	SP-contextual(obj) & question	31.5	0.56	0.60	0.53	0.28	0.91	0.65
Turn on the stove	“carefully turn on the stove”	addition(act)	90.8	0.06	0.00	0.11	0.15	0.33	0.03
	“turn on the range”	SP-habitual(obj)	71.8	0.36	0.34	0.38	0.19	0.41	0.26
	“Is the range hot yet?”	SP-habitual(obj) & hint	33.2	0.65	0.70	0.60	0.40	0.92	0.88
Open the middle drawer of the cabinet	“carefully open the middle drawer of the cabinet”	addition(act)	90.8	0.03	0.00	0.05	0.10	0.12	0.01
	“Find the cabinet, then proceed to open the middle drawer”	coordination	80.2	0.25	0.00	0.50	0.10	0.12	0.01
	“The storage unit’s middle compartment is currently shut”	SP-habitual(obj) & hint	31.6	0.46	0.41	0.50	0.19	0.72	0.49

Table 10: Qualitative comparison of PRIDE, a task-grounded paraphrase distance metric, with general-purpose NLP distance metrics on selected LIBERO-Para examples. Each task group presents three paraphrases of increasing linguistic distance: a minor addition, a lexical substitution, and a compound paraphrase combining object substitution with an indirect speech act. PRIDE increases monotonically as success rate (SR) degrades, reflecting its decomposition into keyword similarity ( $S_K$ ) and structural similarity ( $S_T$ ). In contrast, 1-BERT lacks discriminative range, 1-BLEU fluctuates inconsistently, and 1-METEOR fails to capture structurally induced difficulty when keywords are preserved (e.g., coordination in the third group scores 0.01 despite a 10.6% SR drop).

predominantly trained on.

### Qualitative Comparison with NLP Metrics.

Tab. 10 illustrates how PRIDE captures task-relevant linguistic variation compared to general-purpose NLP metrics. For each task group, we present three paraphrases of increasing difficulty: a minor addition (e.g., prepending “carefully”), a lexical substitution of the object or action, and a compound paraphrase combining object substitution with an indirect speech act. PRIDE increases monotonically as success rate degrades—for instance, in the first group, PRIDE rises from 0.03 to 0.35 to 0.56 as SR drops from 90.8% to 70.3% to 31.5%. This graduated behavior stems from the complementary design of its two components:  $S_K$  remains near zero for syntactic-only changes (e.g., addition) but sharply increases when task-critical keywords are replaced, while  $S_T$  captures structural divergence from the imperative form even when keywords are preserved.

In contrast, conventional NLP metrics each exhibit notable limitations. 1-BERTScore (Zhang et al., 2019) remains in a narrow range (0.10–0.28) across all paraphrase types, failing to distinguish between benign additions and highly disruptive compound paraphrases. 1-BLEU (Papineni et al., 2002) behaves erratically: in the first group, it assigns a higher distance to a simple object substitution (0.80) than the gap between that substitution and a far more disruptive compound form (0.80 → 0.91), compressing meaningful difficulty differences. 1-METEOR (Banerjee and Lavie, 2005) tracks the overall degradation trend more faithfully than the other two metrics, owing to its synonym and stem matching via WordNet (Miller, 1995). However, it still fails to capture structurally induced difficulty: in the third group, coordi-

ination (“Find the cabinet, then proceed to open the middle drawer”) receives the same score as a trivial addition (both 0.01), despite a 10.6 pp SR gap (90.8% → 80.2%), because the original keywords are largely preserved. More fundamentally, METEOR provides only a single scalar distance and cannot decompose *why* a paraphrase is distant—whether due to keyword replacement or structural transformation—limiting its diagnostic utility. PRIDE addresses this through its explicit  $S_K/S_T$  decomposition, enabling researchers to attribute performance degradation to specific linguistic dimensions.

**Quantitative Validation.** Beyond qualitative examples, we verify that PRIDE correlates with actual task performance. Fig. 16 plots the mean success rate of each paraphrase cell against its PRIDE score for all seven models. All models exhibit statistically significant negative correlations (Pearson  $r$  ranging from  $-0.671$  to  $-0.877$ ,  $p < .0001$ ), confirming that higher paraphrase distance consistently leads to lower task success. This validates PRIDE as a meaningful difficulty metric for paraphrase robustness evaluation.

## C Experiment

### C.1 Setup

**Computing Infrastructure.** All experiments were conducted on NVIDIA RTX A6000 and NVIDIA L40S GPUs. Specifically, OpenVLA-OFT variants were evaluated on RTX A6000 GPUs, while all other models (X-VLA, VLA-Adapter,  $\pi_{0.5}$ ,  $\pi_{0.5}$  (expert-only), and Xiaomi-Robotics-0) were evaluated on L40S GPUs. The total evaluation cost across all seven model configurations amounts to approximately **194 GPU hours** (Tab. 11). For  $\pi_{0.5}$  (expert-only), the training was also performed

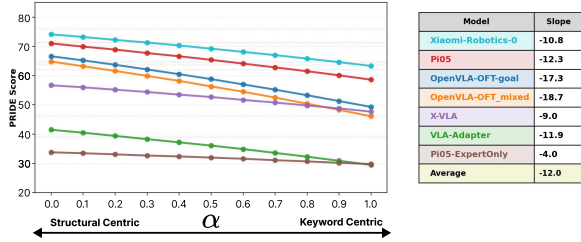


Figure 13: Effect of the weighting parameter  $\alpha$  on PRIDE scores across all models. Left: as  $\alpha$  increases from 0 (structure-centric) to 1 (keyword-centric), PRIDE scores decrease consistently for all models, indicating that keyword-based evaluation assigns higher credit to samples that models already solve easily. Right: per-model linear slope of the PRIDE- $\alpha$  curve. Steeper negative slopes indicate stronger dependence on keyword similarity over structural similarity.

on L40S GPUs following the original  $\pi_{0.5}$  fine-tuning protocol (see Tab. 15 for training hyperparameters and Fig. 15 for the training loss curve).

Model	GPU	VRAM (GB)	Eval Hours
OpenVLA-OFT <sub>goal</sub>	A6000	~16	~12
OpenVLA-OFT <sub>mixed</sub>	A6000	~16	~12
X-VLA	L40S	~6.5	~11
VLA-Adapter	L40S	~3	~11
$\pi_{0.5}$	L40S	~38	~70
$\pi_{0.5}$ (expert-only)	L40S	~38	~70
Xiaomi-Robotics-0	L40S	~14	~8
<b>Total</b>			<b>~194</b>

Table 11: Evaluation GPU hours and peak VRAM usage per model configuration.

**Backbone and Data References.** The VLM backbones used across evaluated models include Prismatic (Karamcheti et al., 2024) with Llama 2 (Touvron et al., 2023), PaliGemma 2 (Steiner et al., 2024), Florence-2 (Xiao et al., 2024), Qwen2.5 (Team, 2024), and Qwen3-VL (Bai et al., 2025). For pre-training data, OpenVLA-OFT uses the Open X-Embodiment (OXE) dataset (O’Neill et al., 2024), and X-VLA is pre-trained on Droid (Khazatsky et al., 2024), RoboMind (Wu et al., 2024), and Agibot (Bu et al., 2025). All  $\pi_{0.5}$  variants use AdamW (Loshchilov and Hutter, 2017) as the optimizer (Tab. 15).

**Model Weights and Code.** All evaluated models use publicly released checkpoints and official codebases, except for  $\pi_{0.5}$  (expert-only), which we fine-tuned from the base  $\pi_{0.5}$  checkpoint by freezing the VLM and updating only the action expert. Tab. 13 summarizes architecture-level specifications, and

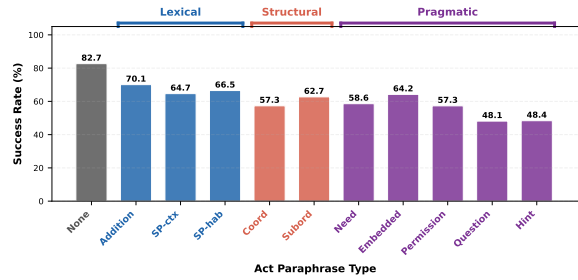


Figure 14: Success rate breakdown by action paraphrase type, averaged across all 7 model configurations. Paraphrase types are grouped into three linguistic categories: **Lexical** (surface-level word changes), **Structural** (syntactic reorganization), and **Pragmatic** (indirect speech acts). Performance degrades progressively from the original instruction (82.7%) through lexical variants (66–70%) and structural variants (57–63%) to the most indirect pragmatic forms such as Question (48.1%) and Hint (48.4%).

Tab. 14 details the fine-tuning configurations. The code repositories and pretrained weights are listed in Tab. 12.

**Evaluation Protocol.** Each model is evaluated across 5 different random seeds (7, 8, 9, 10, 11) per task-paraphrase configuration. All reported success rates represent the **mean over 5 seeds**; standard deviations are not reported, as our analysis focuses on aggregate robustness trends across paraphrase types rather than per-configuration variance. We use the LIBERO simulation environment with its default evaluation settings (i.e., maximum episode length and success criteria) as defined in the original LIBERO benchmark.

## C.2 Result

**Reporting Protocol.** All success rate values reported in this paper are the mean of 5 independent evaluation runs with different random seeds. We do not perform hyperparameter search for evaluation; all models are evaluated using their officially released or documented inference configurations.

## D Analysis

### D.1 Finding 1: Paraphrase Fragility Persists Across Architectures, Data Scales, and Fine-tuning Strategies

Fig. 17 presents per-model success rate heatmaps across all Object  $\times$  Action paraphrase type combinations. While all seven models degrade under object paraphrasing, the degradation manifests in two distinct patterns. OpenVLA-OFT variants

Model	Code	Weights
OpenVLA-OFT <sub>goal</sub>	<a href="https://github.com/moojink/openvla-of-t">https://github.com/moojink/openvla-of-t</a>	<a href="https://huggingface.co/moojink/openvla-7b-of-t-finetuned-libero-goal">https://huggingface.co/moojink/openvla-7b-of-t-finetuned-libero-goal</a>
OpenVLA-OFT <sub>mixed</sub>	(same as above)	<a href="https://huggingface.co/moojink/openvla-7b-of-t-finetuned-libero-spatial-object-goal-10">https://huggingface.co/moojink/openvla-7b-of-t-finetuned-libero-spatial-object-goal-10</a>
$\pi_{0.5}$ (expert-only)	<a href="https://github.com/Physical-Intelligence/openpi">https://github.com/Physical-Intelligence/openpi</a> (JAX)	<a href="gs://openpi-assets/checkpoints/pi05_libero">gs://openpi-assets/checkpoints/pi05_libero</a>
X-VLA	<a href="https://github.com/huggingface/lerobot">https://github.com/huggingface/lerobot</a>	<a href="https://huggingface.co/lerobot/xvla-libero">https://huggingface.co/lerobot/xvla-libero</a>
VLA-Adapter	<a href="https://github.com/OpenHelix-Team/VLA-Adapter">https://github.com/OpenHelix-Team/VLA-Adapter</a>	<a href="https://huggingface.co/VLA-Adapter/LIBERO-Goal-Pro">https://huggingface.co/VLA-Adapter/LIBERO-Goal-Pro</a>
Xiaomi-Robotics-0	<a href="https://github.com/XiaomiRobotics/Xiaomi-Robotics-0">https://github.com/XiaomiRobotics/Xiaomi-Robotics-0</a>	<a href="https://huggingface.co/XiaomiRobotics/Xiaomi-Robotics-0-LIBERO">https://huggingface.co/XiaomiRobotics/Xiaomi-Robotics-0-LIBERO</a>

Table 12: Code repositories and pretrained weight sources for all evaluated models.

Model	Release	Arch. Type	VLM Backbone	VLM Params	Action Module	Action Params	Total Params
OpenVLA-OFT	2025.03	Parallel Decoding	Prismatic (Llama 2)	7B	L1 MLP	<1M	7.5B
$\pi_{0.5}$	2025.09	VLM + Action Expert	PaliGemma 2	3B	Flow matching expert	0.3B	3.3B
VLA-Adapter	2025.09	Bridge-based	Prismatic (Qwen2.5-0.5B)	0.5B	Bridge Attention Policy	97M	0.6B
X-VLA	2026.01	Soft-prompted	Florence-2	0.5B	Flow matching transformer	~0.4B	0.9B
Xiaomi-Robotics-0	2026.02	VLM + Action Expert	Qwen3-VL-4B	4B	Flow matching DiT	~0.7B	4.7B

Table 13: Architecture-level specifications of the evaluated VLA models. Release denotes the public code release date (YYYY.MM). Models span a range of architectural paradigms—from parallel decoding to bridge-based adapters to flow matching action experts—with total parameter counts ranging from 0.6B to 7.5B. OpenVLA-OFT variants (goal/mixed) share the same architecture and are listed as a single entry.

and VLA-Adapter exhibit a sharp cliff between object-preserved rows (None, Addition) and object-paraphrased rows (SP-contextual, SP-habitual)—the top two rows remain nearly uniformly green while the bottom two rows shift abruptly to red. This two-band pattern directly reflects the large preserved-vs-paraphrased gaps reported in Fig. 7: OpenVLA-OFT<sub>goal</sub> (48.3 pp), OpenVLA-OFT<sub>mixed</sub> (51.0 pp), and VLA-Adapter (37.1 pp) all show a clear visual boundary at the object paraphrasing threshold. In contrast,  $\pi_{0.5}$ , X-VLA, and Xiaomi-Robotics-0 display a more gradual degradation across both axes without a single sharp boundary, consistent with their comparatively smaller preserved-vs-paraphrased gaps (19.8–35.7 pp).

Despite these differences in degradation profile, the conclusion is shared: every model falls below 50% in the most challenging compound cells, confirming that paraphrase fragility is universal regardless of architecture.

## D.2 Finding 2: Object Grounding Is the Primary Bottleneck

**Alpha Sensitivity Analysis.** Fig. 13 examines how the balance between the two PRIDE components—keyword similarity ( $S_K$ ) and structural similarity ( $S_T$ )—affects the overall robustness score. As  $\alpha$  shifts toward 1.0 (keyword-centric), PRIDE scores decrease across all models, revealing that models generally succeed on samples where keywords are preserved and fail when keywords are paraphrased. Conversely, as  $\alpha$  approaches 0.0 (structure-centric), scores rise uniformly, suggesting that structural variation alone is less disruptive than keyword replacement. This confirms that

object-level keyword changes, rather than syntactic reformulations, are the dominant factor driving success rate degradation across current VLA architectures.

The per-model slopes in the right panel of Fig. 13 further reveal architecture-specific sensitivities. OpenVLA-OFT<sub>goal</sub> and OpenVLA-OFT<sub>mixed</sub> exhibit the steepest slopes (−17.3 and −18.7, respectively), consistent with the large success rate gaps between object-preserved and object-paraphrased conditions reported in Fig. 7 (48.3pp and 51.0pp, respectively). Their high keyword dependence indicates that these models rely heavily on exact object noun matching for task execution.

Interestingly, at  $\alpha \geq 0.9$ , X-VLA overtakes OpenVLA-OFT<sub>mixed</sub> in PRIDE score, indicating that despite lower structural robustness overall, X-VLA is more resilient to keyword-level variation. Similarly,  $\pi_{0.5}$  (expert-only) closes the gap with VLA-Adapter at  $\alpha = 1.0$ , suggesting relatively stronger keyword robustness despite its lower absolute performance. These crossover patterns demonstrate the diagnostic utility of  $\alpha$ -tuning: by adjusting the weighting, practitioners can identify which robustness dimension—keyword preservation or structural flexibility—a given model excels at, informing model selection for deployment environments where one linguistic dimension may be more prevalent than the other.

**Action Indirectness.** Fig. 14 breaks down success rate by action paraphrase type across all models. Lexical-level changes (Addition, SP-contextual, SP-habitual) cause moderate degradation (66–70%), while structural reorganizations

Model	Pre-train	LIBERO Data	Fine-tune (Domain Adaptation)		Weights
	Pre-train Data		FT Method	FT Scope	
OpenVLA-OFT <sub>goal</sub>	OXE (970k traj)	Goal only	LoRA (r=32)	All modules	Released
OpenVLA-OFT <sub>mixed</sub>	OXE (970k traj)	All 4 suites	LoRA (r=32)	All modules	Released
$\pi_{0.5}$	Proprietary + open (10K+ hrs)	All 4 suites	Full	All modules	Released
$\pi_{0.5}$ (expert-only)	Proprietary + open (10K+ hrs)	All 4 suites	Full	Action Expert only	Ours
VLA-Adapter	No robotic pretrain	Goal only	LoRA (r=64)	All modules	Released
X-VLA	Droid + Robomind + Agibot (290k)	All 4 suites	LoRA (r=64)	All modules	Released
Xiaomi-Robotics-0	Open + in-house (~200M steps)	All 4 suites	Full	All modules	Released

Table 14: LIBERO fine-tuning configurations of the evaluated VLA models. All models are fine-tuned on LIBERO and evaluated on LIBERO-Para. “Released” denotes publicly available checkpoints; “Ours” denotes checkpoints fine-tuned by us following the original training protocol (see Fig. 15 for the training loss curve). Models trained on “All 4 suites” use the mixed configuration of LIBERO-Goal, LIBERO-Spatial, LIBERO-Object, and LIBERO-Long. Note that  $\pi_{0.5}$  (expert-only) freezes the vision-language backbone and updates only the action expert.

	$\pi_{0.5}$	$\pi_{0.5}$ (expert-only)
VLM (img + llm)	Fine-tuned	Frozen
Action Expert	Fine-tuned	Fine-tuned
Trainable Params	~3.3B	~300M
Batch Size	256	256
Peak LR	5e-5	5e-5
Optimizer	AdamW (grad clip 1.0)	AdamW (grad clip 1.0)
EMA Decay	0.999	0.999
Warmup Steps	10k	10k
Training Steps	30k	30k
Action Horizon	10	10

Table 15: Training configurations for  $\pi_{0.5}$  variants. The expert-only variant freezes the VLM and fine-tunes only the Action Expert.

(Coordination, Subordination) reduce success further to around 57–63%. The sharpest drops occur in the pragmatic category, where Question and Hint—forms that require pragmatic inference to recover the underlying imperative—bring success down to ~48%.

Notably, the overall action-axis degradation is milder than the object-axis degradation reported in Sec. 6.2. We attribute this to the constrained nature of tabletop manipulation: the action space is limited to a small set of motor primitives (pick, place, push, open, etc.), and each object typically affords only a narrow range of feasible actions (e.g., *stove* → *turn on*). This low action ambiguity allows models to converge on the correct primitive even under moderate linguistic variation. However, when the directive intent itself becomes opaque—as in questions or hints—models can no longer reliably extract the intended action, leading to the steep drop in the pragmatic category.

**LIBERO-Goal Instructions.** LIBERO-Goal instructions refer to each object by a single fixed reference throughout all tasks. As shown in Fig. 12, objects such as *stove*, *bowl*, and *rack* appear con-

sistently under the same surface form, with no synonym or alternative reference used in any instruction. Because models are fine-tuned exclusively on these fixed references, they are never exposed to lexical variation in object references during training. This single-reference convention likely reinforces surface-level keyword matching and contributes to the sharp performance drops observed when object nouns are replaced with semantically equivalent alternatives in LIBERO-Para.

### D.3 Finding 3: Failures Are Predominantly Planning-Level, Not Execution-Level

**DTW-Based Trajectory Classification.** We classify each failed episode as Near-GT (execution-level) or Far-GT (planning-level) based on its Dynamic Time Warping (DTW) distance to a pseudo ground-truth (GT) trajectory, as formalized in Algorithm 1.

**Why DTW.** Trajectory lengths vary across episodes—successful episodes may terminate early while failed episodes often run to the maximum step limit. Euclidean distance requires fixed-length inputs and cannot account for temporal misalignment between trajectories that follow similar spa-

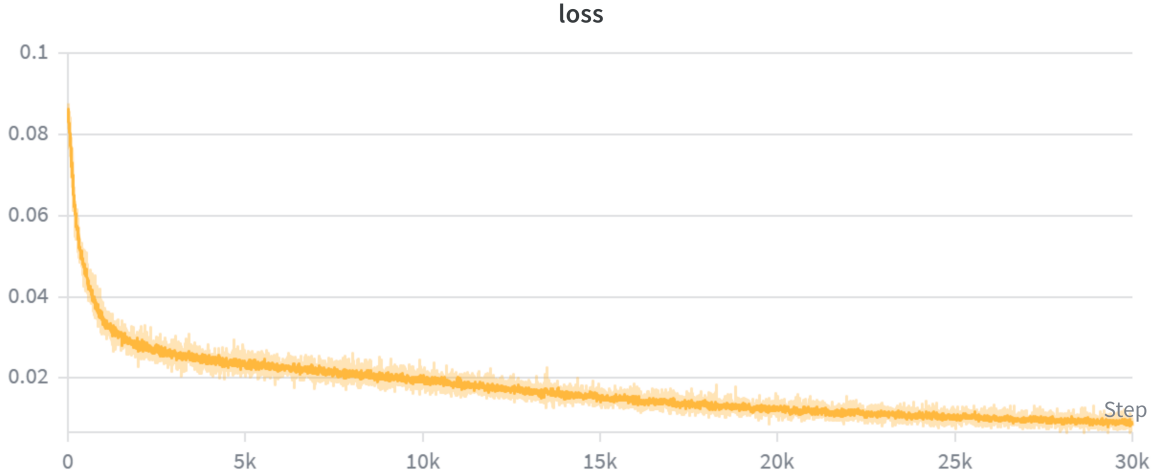


Figure 15: Training loss curve of  $\pi_{0.5}$  (expert-only) fine-tuned on LIBERO. The model is trained for 30K steps, matching the original training configuration. The loss converges around 15K steps, indicating stable training completion.

Near-GT % of Total					Far-GT % of Total				
Model	max	p99	p95	p90	Model	max	p99	p95	p90
OpenVLA-OFT <sub>goal</sub>	1.6	1.4	0.4	0.3	OpenVLA-OFT <sub>goal</sub>	33.7	33.9	34.9	35.0
OpenVLA-OFT <sub>mixed</sub>	3.3	1.0	0.1	0.0	OpenVLA-OFT <sub>mixed</sub>	33.0	35.3	36.2	36.3
$\pi_{0.5}$	2.4	1.0	0.6	0.3	$\pi_{0.5}$	26.2	27.6	28.0	28.3
$\pi_{0.5}$ (expert-only)	12.5	6.2	2.1	0.9	$\pi_{0.5}$ (expert-only)	48.4	54.7	58.8	60.0
VLA-Adapter	4.2	2.2	0.5	0.0	VLA-Adapter	49.5	51.5	53.2	53.7
X-VLA	5.2	2.9	0.8	0.4	X-VLA	32.7	35.0	37.1	37.5
Xiaomi-Robotics-0	1.8	0.3	0.1	0.0	Xiaomi-Robotics-0	22.2	23.7	23.9	24.0

Table 16:  $\tau$  threshold ablation for trajectory-based failure classification. “max” denotes the most lenient threshold (widest Near-GT boundary); p99, p95, and p90 progressively tighten the criterion. Across all thresholds, Far-GT (planning-level) failures consistently dominate, confirming that the finding is robust to threshold selection.

tial paths at different speeds. DTW handles both variable-length sequences and temporal warping, making it suitable for comparing manipulation trajectories. We use `fastdtw` (Salvador and Chan, 2007) with Euclidean distance as the local cost function, and normalize the resulting distance by sequence length to ensure comparability across episodes.

**Resampling.** To standardize input length for DTW, all trajectories are resampled to  $K=50$  points via linear interpolation. This value was chosen as a practical trade-off between spatial resolution and computational cost across  $\sim 143K$  total episodes ( $4,092$  paraphrases  $\times 5$  seeds  $\times 7$  models).

**EEF Position Only.** From the 7-dimensional proprioceptive state  $(x, y, z, r_x, r_y, r_z, g)$ , we use only the first three dimensions corresponding to the end-effector (EEF) absolute position  $(x, y, z)$ . The re-

maining dimensions (orientation, gripper state) are excluded because spatial trajectory divergence is the most direct indicator of whether the model planned toward the correct target object—the core diagnostic question of this analysis.

**Threshold Robustness.** The threshold  $\tau_t$  is set per-task as the maximum DTW distance among successful episodes (Algorithm 1, line 12), representing the most lenient Near-GT boundary. To verify that our findings are not sensitive to this choice, we repeat the classification with progressively stricter thresholds (p99, p95, p90 of successful DTW distances). As shown in Tab. 16, Far-GT failures remain dominant across all thresholds—tightening  $\tau$  shifts some Near-GT episodes to Far-GT but does not alter the overall conclusion. For example, even under the strictest criterion (p90),  $\pi_{0.5}$  (expert-only) retains the highest Near-GT ratio among all models, consistent with the frozen-VLM

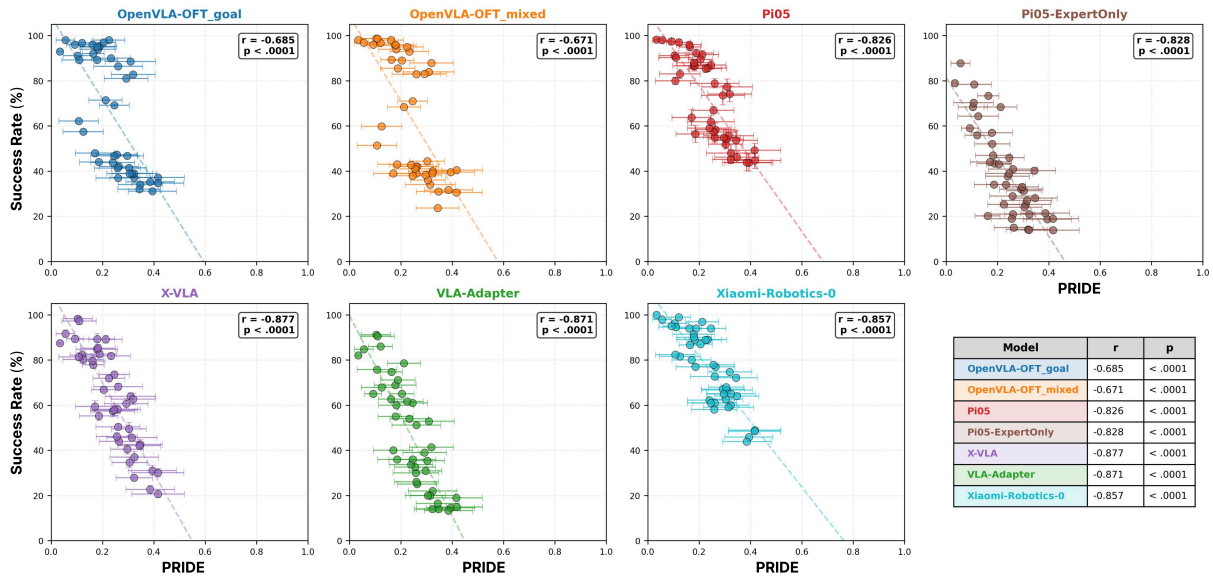


Figure 16: Correlation between PRIDE score (PD) and success rate (SR) for each VLA model on LIBERO-Para. Each point represents the mean SR of a paraphrase cell, with error bars indicating standard deviation. Colors are unified per model for visual clarity. All models exhibit statistically significant negative correlations ( $p < .0001$ ), with Pearson  $r$  values ranging from  $-0.671$  to  $-0.877$ , validating that higher paraphrase distance consistently leads to lower task success. The summary table (bottom right) reports  $r$  and  $p$  for all models.

interpretation discussed in Sec. 6.3.

**GT Trajectory Consistency.** Fig. 18 visualizes successful EEF trajectories for each LIBERO-Goal task. Within each task, successful trajectories converge to a narrow spatial corridor with low variance, validating the use of their mean as a pseudo GT. This consistency arises from the LIBERO-Goal training data, which contains a single fixed demonstration path per task with no route diversity.

**Per-Model Failure Decomposition.** Fig. 19 provides a fine-grained view of the failure classification from Tab. 4, decomposed along the Object and Action axes for each model individually. Two observations are consistent across all models. First, Near-GT (execution-level) failures account for a small fraction in every category, confirming that the dominance of Far-GT failures reported in Sec. 6.3 is not an artifact of aggregation but holds at the per-type level. Second, Near-GT failures do not concentrate along any particular paraphrase axis or type—they are distributed roughly uniformly, suggesting that execution-level errors are not systematically triggered by specific linguistic properties.

The sole exception is  $\pi_{0.5}$  (expert-only), which shows elevated Near-GT ratios across most categories. As discussed in Sec. 6.1, this model freezes the VLM during fine-tuning, preserving pretrained language understanding that enables partial task

identification. However, the unadapted action expert lacks the precision to convert correct plans into successful executions, resulting in trajectories that track the GT path but ultimately fail.

These patterns reinforce the conclusion that paraphrase robustness improvements should target the instruction-to-task identification stage—where Far-GT failures originate—rather than low-level motor control refinement.

## E AI Assistants

During the course of this work, we used Google’s Gemini 2.5 Pro (<https://gemini.google.com/>) (Comanici et al., 2025) for generating paraphrase candidates in the LIBERO-Para benchmark construction. All generated paraphrases were manually reviewed and filtered by the authors. Additionally, we used AI assistants including OpenAI’s ChatGPT (<https://chatgpt.com/>) (OpenAI, 2023) and Anthropic’s Claude (<https://claude.ai/>) (Anthropic, 2025) to proofread and improve the clarity of our writing. We affirm that these tools served solely as assistive aids and did not contribute to core research ideas, experimental design, analysis, or interpretation of results. The final scientific content and all claims made in this paper are the sole responsibility of the authors.

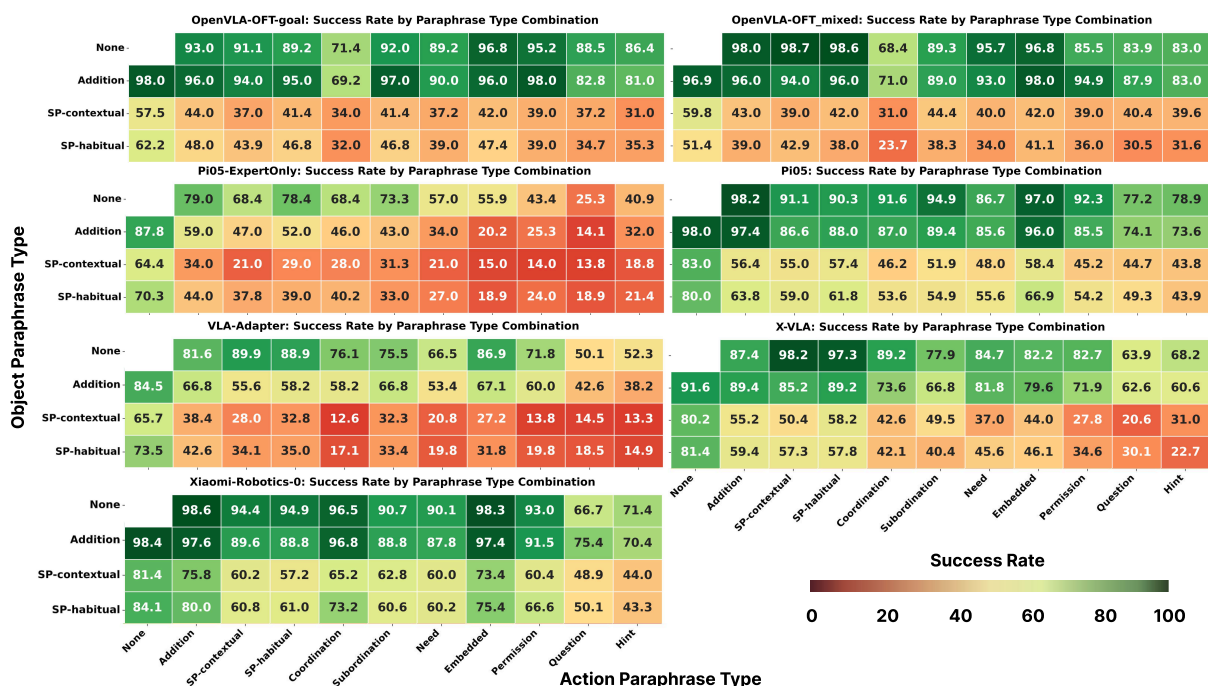


Figure 17: Per-model success rate heatmaps across all Object  $\times$  Action paraphrase type combinations on LIBERO-Para. Rows represent object paraphrase types and columns represent action paraphrase types. Each cell reports the mean success rate over 5 seeds. The None row/column indicates the original (unparaphrased) instruction. All models show consistent degradation as paraphrase distance increases from the top-left (original) to the bottom-right (most distant) cells.

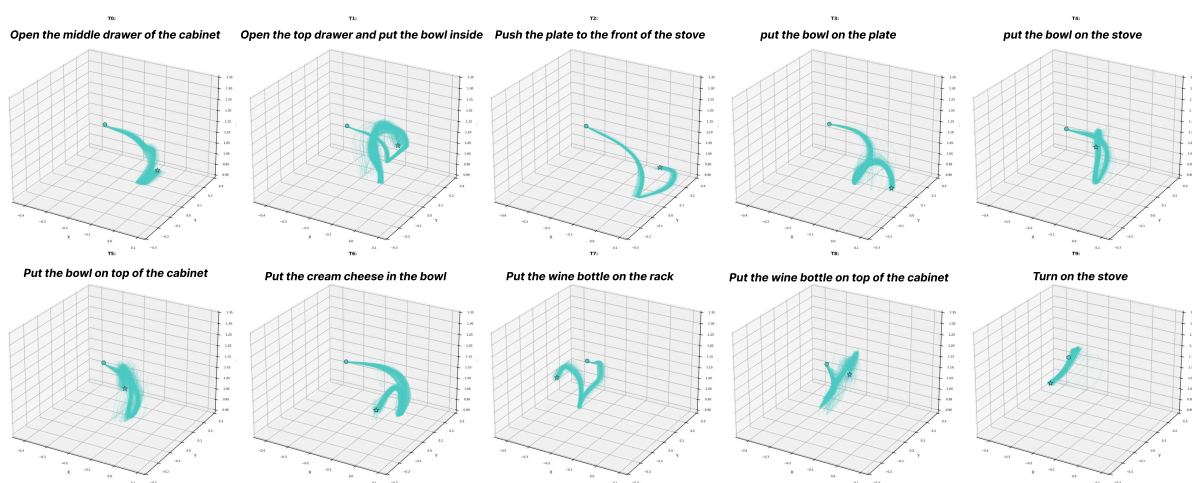


Figure 18: Successful EEF trajectories of Xiaomi-Robotics-0 on LIBERO-Para, grouped by LIBERO-Goal task index (T0–T9). Within each task, successful trajectories converge to a narrow corridor with low spatial variance, indicating that manipulation strategies are largely invariant to paraphrase variation. We observe consistent patterns across all evaluated models; a single model is shown for visual clarity. This consistency motivates the use of the mean successful trajectory as a pseudo ground-truth (GT) in Algorithm 1.

### Near-GT / Far-GT Failure Analysis per Model

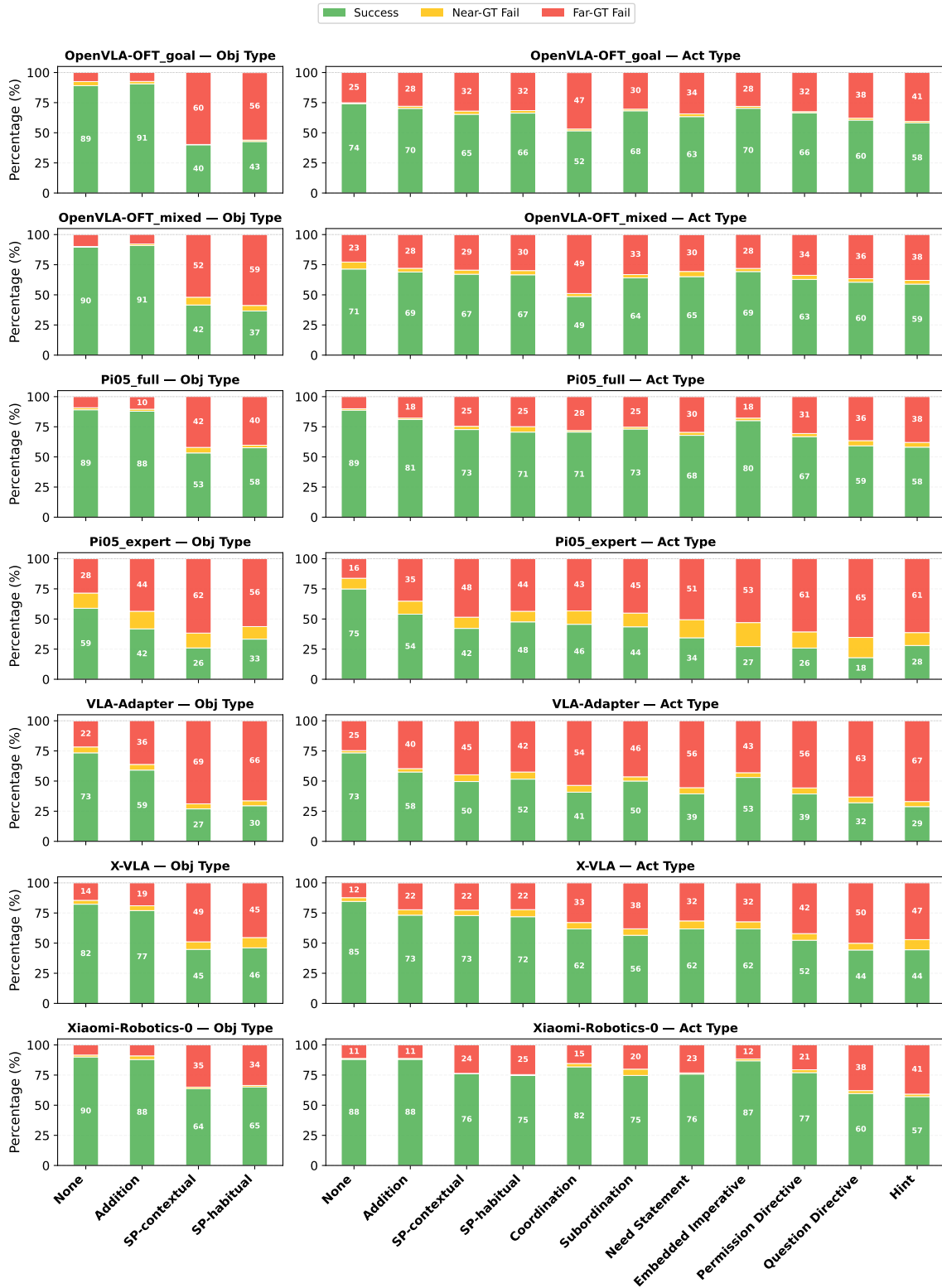


Figure 19: Near-GT / Far-GT failure breakdown per model, decomposed by Object axis (left) and Action axis (right). Each bar shows the proportion of Success (green), Near-GT failure (yellow, execution-level), and Far-GT failure (red, planning-level) episodes. The threshold  $\tau$  is set to the maximum DTW distance among successful episodes per task. Across all models and paraphrase types, Far-GT failures consistently dominate, with no concentration of Near-GT failures along any specific axis. The exception is  $\pi_{0.5}$  (expert-only), which exhibits a higher Near-GT ratio due to its frozen VLM preserving partial task identification while the unadapted action expert fails at execution.



---

**Algorithm 1** Trajectory-based failure classification for Sec. 6.3 A pseudo ground-truth trajectory (GT) is constructed from successful episodes of each model on LIBERO-Para. Failed episodes are classified as Near-GT (execution-level) or Far-GT (planning-level) based on DTW distance, with the threshold  $\tau_t$  set to the maximum distance among successes.

---

**Require:** Set of episodes  $\mathcal{E} = \{e_1, \dots, e_N\}$  for original LIBERO-Goal task index  $t \in \{0, 1, \dots, 9\}$ , each with trajectory  $\tau_i \in \mathbb{R}^{T_i \times 3}$  and outcome  $s_i \in \{0, 1\}$ ; resampling size  $K=50$

**Ensure:** Classification of each failed episode as NEAR-GT or FAR-GT

**// Step 1: Partition episodes**

- 1:  $\mathcal{S}_t \leftarrow \{e_i \in \mathcal{E} \mid s_i = 1\}$  ▷ successes
- 2:  $\mathcal{F}_t \leftarrow \{e_i \in \mathcal{E} \mid s_i = 0\}$  ▷ failures

**// Step 2: Construct pseudo-GT trajectory**

- 3: **for** each  $e_i \in \mathcal{S}_t$  **do**
- 4:    $\hat{\tau}_i \leftarrow \text{RESAMPLE}(\tau_i[:, : 3], K)$  ▷ first 3 dims of proprio: EEF absolute position (x,y,z)
- 5: **end for**
- 6:  $\tau^{\text{GT}} \leftarrow \frac{1}{|\mathcal{S}_t|} \sum_{e_i \in \mathcal{S}_t} \hat{\tau}_i$

**// Step 3: Compute DTW distances**

- 7:  $L_{\max} \leftarrow \max_{e_j \in \mathcal{S}_t} T_j$
- 8: **for** each  $e_i \in \mathcal{F}_t$  **do**
- 9:    $\tau'_i \leftarrow \text{RESAMPLE}(\tau_i[:, L_{\max}, : 3], K)$
- 10:    $d_i \leftarrow \text{DTW}(\tau'_i, \tau^{\text{GT}})$  ▷ DTW: Dynamic Time Warping
- 11: **end for**

**// Step 4: Threshold**

- 12:  $\tau_t \leftarrow \max_{e_i \in \mathcal{S}_t} d_i$

**// Step 5: Classify failures**

- 13: **for** each  $e_i \in \mathcal{F}_t$  **do**
  - 14:   **if**  $d_i \leq \tau_t$  **then**
  - 15:      $\text{LABEL}(e_i) \leftarrow \text{NEAR-GT}$  ▷ execution-level
  - 16:   **else**
  - 17:      $\text{LABEL}(e_i) \leftarrow \text{FAR-GT}$  ▷ planning-level
  - 18:   **end if**
  - 19: **end for**
  - 20: **return**  $\{\text{LABEL}(e_i)\}_{e_i \in \mathcal{F}_t}$
-

### Generator Prompt

Paraphrase the given robot manipulation instruction while preserving semantic meaning.

#### Rules:

- Preserve plurality (singular/plural must match original)
- Do not add visual attributes (color, size, shape, material)
- Do not add spatial attributes (position, location, direction)
- Modify only what is specified in the task guidelines below

#### Scope:

- Object tasks: modify only object nouns, preserve verbs and structure
- Action tasks: modify only action elements, preserve object nouns

**Output:** One paraphrase per line. No explanations or alternatives.

Figure 20: Common prompt template for the Paraphrase Generator (LLM), shared across all paraphrase types.

### Verifier Prompt

#### Criteria:

- Task compliance: Required transformations applied, prohibited changes avoided.
  - Object tasks (obj\_\*): only object nouns changed, verbs/structure intact
  - Action tasks (act\_\*): only action elements changed, object nouns intact
- Semantic preservation: Core action and target objects unchanged.
- Naturalness: Grammatically correct, natural phrasing.
- Format: Single instruction only, no meta-commentary or explanations.
- Lexical clarity: Avoid confusion with environment objects (stove, bowl, plate, rack, wine bottle, cream cheese, cabinet).
  - Acceptable: “cupboard” (distinct from cabinet)
  - Reject: “dish” (confusable with plate/bowl)

**Output:** Accepted paraphrases only, one per line.

Figure 21: Common prompt template for the Paraphrase Verifier (LLM), used to filter generated paraphrases.

### Merge Generator Prompt

Merge object paraphrases and action paraphrases into combined variants.

**Input:**

- Original instruction
- Object paraphrase examples (nouns changed)
- Action paraphrase examples (verbs/structure changed)

**Task:** Create paraphrases with both object and action modifications applied.

**Process:**

1. Identify object substitution patterns (e.g., “drawer” → “compartment”)
2. Identify action modification patterns (e.g., “pick” → “grab”)
3. Apply both transformations coherently

**Example:**

- Original: “*pick the bowl and place on the stove*”
- Object variant: “*pick the container and place on the cooktop*”
- Action variant: “*grab the bowl and put on the stove*”
- Merged: “*grab the container and put on the cooktop*”

**Output:** 5–10 merged paraphrases, one per line. No numbering or explanations.

Figure 22: Prompt template for combining validated Object and Action paraphrases into merged variants.

### Merge Verifier Prompt

Evaluate merged paraphrases that combine object and action changes.

**Criteria:**

- Completeness: Both object nouns AND action elements must differ from original. Reject if only one type changed.
- Pattern consistency: Changes follow the provided examples.
- Semantic preservation: Task intent and outcome unchanged.
- Naturalness: Grammatically correct, coherent combination.
- Format: Single instruction, no meta-commentary.
- Lexical clarity: No confusion with environment objects.

**Output:** Accepted paraphrases only, one per line.

Figure 23: Prompt template for verifying merged paraphrases before final inclusion in the dataset.

## Object-Lexical Types Prompts

### **obj\_lexical\_same\_polarity\_habitual**

Replace object nouns with general synonyms.

EPT: Same-polarity substitution (habitual)

#### **Guidelines:**

- Use commonly accepted synonyms (bowl → cup, cabinet → cupboard)
- Preserve grammatical form
- Keep verbs and structure unchanged

#### **Examples:**

- *“Pick the bowl and place on the stove” → “Pick the cup and place on the stove.”*
- *“Open the middle layer of drawer” → “Open the middle layer of compartment.”*

---

### **obj\_lexical\_same\_polarity\_contextual**

Replace object nouns with contextually appropriate alternatives.

EPT: Same-polarity substitution (contextual)

#### **Guidelines:**

- Use contextually similar items (bowl → container, stove → cooking surface)
- Maintain semantic appropriateness for manipulation tasks
- Preserve structure

#### **Examples:**

- *“Pick the bowl and place on the stove” → “Pick the container and place on the cooking surface.”*
- *“Open the middle layer of drawer” → “Open the middle tier of drawer.”*

---

### **obj\_lexical\_addition**

Add functional descriptors from object names.

EPT: Addition

#### **Guidelines:**

- Add functional/categorical adjectives (soup bowl, kitchen cabinet)
- Exclude visual adjectives (color, size, material)
- Exclude spatial adjectives (top, left, big)
- Preserve plurality

#### **Examples:**

- *“Pick the bowl and place on the stove” → “Pick the mixing bowl and place on the kitchen stove.”*
- *“Open the middle layer of drawer” → “Open the middle layer of storage drawer.”*

Figure 24: Type-specific generation guidelines for Object-Lexical paraphrases. These guidelines are provided to the Generator for paraphrase generation and also appended to the Verifier to assess whether the generated output conforms to the intended variation type.

## Action-Lexical Types Prompts

### **act\_lexical\_same\_polarity\_habitual**

Replace action verbs with general synonyms.

EPT: Same-polarity substitution (habitual)

#### **Guidelines:**

- Use common verb synonyms (pick → grab, place → put)
- Preserve structure and arguments
- Keep object nouns unchanged

#### **Examples:**

- *“Pick the bowl and place on the stove”* → *“Grab the bowl and put on the stove.”*
  - *“Open the middle layer of drawer”* → *“Pull the middle layer of drawer.”*
- 

### **act\_lexical\_same\_polarity\_contextual**

Replace action verbs with contextually appropriate alternatives.

EPT: Same-polarity substitution (contextual)

#### **Guidelines:**

- Use context-appropriate alternatives (pick → grasp, place → position)
- Preserve core action meaning
- Keep object nouns unchanged

#### **Examples:**

- *“Pick the bowl and place on the stove”* → *“Grasp the bowl and position on the stove.”*
  - *“Open the middle layer of drawer”* → *“Access the middle layer of drawer.”*
- 

### **act\_lexical\_addition\_deletion**

Add or remove manner adverbs.

EPT: Addition/Deletion

#### **Guidelines:**

- Add single-word adverbs (carefully, gently, slowly)
- For phrasal additions, use act\_structural\_ellipsis instead
- Keep verb and structure unchanged

#### **Examples:**

- *“Pick the bowl and place on the stove”* → *“Carefully pick the bowl and place on the stove.”*
- *“Open the middle layer of drawer”* → *“Gently open the middle layer of drawer.”*

Figure 25: Type-specific generation guidelines for Action-Lexical paraphrases. These guidelines are provided to the Generator for paraphrase generation and also appended to the Verifier to assess whether the generated output conforms to the intended variation type.

## Action-Structural Types Prompts

### **act\_structural\_coordination**

Modify coordination structure.

EPT: Coordination changes (syntax-based)

#### **Guidelines:**

- Split into separate sentences
- Add explicit ordering (First... then...)
- Combine with coordination
- Preserve all information

#### **Examples:**

- *“Pick the bowl and place on the stove”* → *“Pick the bowl. Place it on the stove.”*
- *“Open the middle layer of drawer”* → *“Locate the drawer, then open the middle layer.”*

---

### **act\_structural\_subordination**

Modify subordination structure.

EPT: Subordination changes (syntax-based)

#### **Guidelines:**

- Convert coordination to subordination
- Use temporal subordinators (after, once, when)
- Use purpose subordinators (so that, in order to)
- Preserve semantic relations

#### **Examples:**

- *“Pick the bowl and place on the stove”* → *“After picking the bowl, place it on the stove.”*
- *“Open the middle layer of drawer”* → *“Open the middle layer of drawer in order to access the contents.”*

Figure 26: Type-specific generation guidelines for Action-Structural paraphrases. These guidelines are provided to the Generator for paraphrase generation and also appended to the Verifier to assess whether the generated output conforms to the intended variation type.

## Action-Pragmatic Types Prompts (1/2)

### **act\_pragmatical\_need\_statement**

Express as speaker's need.

Ervin-Tripp Type 1: Need Statements

#### **Guidelines:**

- Convert to first-person need (I need, I want, I require)
- Focus on desired outcome rather than process
- Preserve core action and objects

#### **Examples:**

- *“Pick the bowl and place on the stove”* → *“I need the bowl placed on the stove.”*
  - *“Open the middle layer of drawer”* → *“I want the middle layer of drawer open.”*
- 

### **act\_pragmatical\_embedded\_imperative**

Embed in question frame with modals.

Ervin-Tripp Type 3: Embedded Imperatives

#### **Guidelines:**

- Use modal questions (Could you, Would you, Can you)
- Keep agent and action explicit but softened

#### **Examples:**

- *“Pick the bowl and place on the stove”* → *“Could you pick the bowl and place it on the stove?”*
  - *“Open the middle layer of drawer”* → *“Can you open the middle layer of drawer?”*
- 

### **act\_pragmatical\_permission\_directive**

Frame as permission request.

Ervin-Tripp Type 4: Permission Directives

#### **Guidelines:**

- Request permission or access (May I have, Can I have access to)
- Focus on speaker's access requiring hearer's action

#### **Examples:**

- *“Pick the bowl and place on the stove”* → *“May I have the bowl placed on the stove?”*
- *“Open the middle layer of drawer”* → *“Can I have access to the middle layer of drawer?”*

Figure 27: Type-specific generation guidelines for Action-Pragmatic paraphrases (a). These guidelines are provided to the Generator for paraphrase generation and also appended to the Verifier to assess whether the generated output conforms to the intended variation type.

## Action-Pragmatic Types Prompts (2/2)

### **act\_pragmatical\_question\_directive**

Pose information question implying action.

Ervin-Tripp Type 5: Question Directives

#### **Guidelines:**

- Ask contextually relevant question
- Do not explicitly specify desired act
- Action inferred from context

#### **Examples:**

- *“Pick the bowl and place on the stove”* → *“Is the bowl still sitting on the counter?”*
- *“Open the middle layer of drawer”* → *“Do we know the contents of the middle layer of drawer?”*

---

### **act\_pragmatical\_hint**

Make statement implying action through inference.

Ervin-Tripp Type 6: Hints

#### **Guidelines:**

- Use general statement, not surface directive
- State condition or desired state
- Rely on situational inference
- Do not mention action directly

#### **Examples:**

- *“Pick the bowl and place on the stove”* → *“The stove surface is now clear for the bowl.”*
- *“Open the middle layer of drawer”* → *“The middle layer of drawer is still closed.”*

Figure 28: Type-specific generation guidelines for Action-Pragmatic paraphrases (b), continued. These guidelines are provided to the Generator for paraphrase generation and also appended to the Verifier to assess whether the generated output conforms to the intended variation type.